

Occupant Pre-Crash Kinematics in Rotated Seat Arrangements

Diederich, A., Bastien, C., Ekambaram, K. & Wilson, A.

Author post-print (accepted) deposited by Coventry University's Repository

Original citation & hyperlink:

Diederich, A, Bastien, C, Ekambaram, K & Wilson, A 2021, 'Occupant Pre-Crash Kinematics in Rotated Seat Arrangements', Proceedings of the Institution of Mechanical Engineers, Part D: Journal of Automobile Engineering,.
<https://dx.doi.org/10.1177/09544070211004504>

DOI 10.1177/09544070211004504

ISSN 0954-4070

ESSN 2041-2991

Publisher: SAGE Publications

Copyright © and Moral Rights are retained by the author(s) and/ or other copyright owners. A copy can be downloaded for personal non-commercial research or study, without prior permission or charge. This item cannot be reproduced or quoted extensively from without first obtaining permission in writing from the copyright holder(s). The content must not be changed in any way or sold commercially in any format or medium without the formal permission of the copyright holders.

This document is the author's post-print version, incorporating any revisions agreed during the peer-review process. Some differences between the published version and this version may remain and you are advised to consult the published version if you wish to cite from it.

Occupant Pre-Crash Kinematics in Rotated Seat Arrangements

A. Diederich*, C. Bastien*, K. Ekambaram*, A. Wilson*

**Institute for Future Transport and Cities (IFTC), Coventry University, Priory Street, Coventry, CV1 5FB, UK*

Abstract: The introduction of automated L5 driving technologies will revolutionise the design of vehicle interiors and seating configurations, improving occupant comfort and experience. It is foreseen that pre-crash emergency braking and swerving manoeuvres will affect occupant posture, which could lead to an interaction with a deploying airbag. This research addresses the urgent safety need of defining the occupant's kinematics envelope during that pre-crash phase, considering rotated seat arrangements and different seatbelt configurations. The research used two different sets of volunteer tests experiencing L5 vehicle manoeuvres, based in the first instance on 22 50th percentile fit males wearing a lap-belt (OM4IS), while the other dataset is based on 87 volunteers with a BMI range of 19 to 67kg/m² wearing a 3-point belt (UMTRI). Unique biomechanics kinematics corridors were then defined, as a function of belt configuration and vehicle manoeuvre, to calibrate an Active Human Model (AHM) using a multi-objective optimisation coupled with a Correlation and Analysis (CORA) rating. The research improved the AHM omnidirectional kinematics response over current state of the art in a generic lap-belted environment. The AHM was then tested in a rotated seating arrangement under extreme braking, highlighting that maximum lateral and frontal motions are comparable, independent of the belt system, while the asymmetry of the 3-point belt increased the occupant's motion towards the seatbelt buckle. It was observed that the frontal occupant kinematics decrease by 200mm compared to a lap-belted configuration. This improved omnidirectional AHM is the first step towards designing safer future L5 vehicle interiors.

Keywords: Occupant Envelope; Pre-Crash Kinematics; Rotated Seating; Out-of-Position; Automated Driving; Active Human Model

Highlights:

- In vehicle kinematics corridors describing occupant's motion wearing a lap-belt
- In vehicle kinematics corridors describing occupant's motion wearing a 3-point belt
- Omnidirectional activation parameters for the Simcenter Madymo AHM Version 3
- Head kinematics' envelope for emergency braking for rotated seat arrangement

1 Introduction

During the last decades, the introduction of passive occupant safety systems, like seat belts and airbags, helped to significantly reduce the number of fatalities and serious injuries on the road [1]. Today's restraint systems are designed and optimised on standards and strict protocols which are assessing the vehicle's safety performance against the injury criteria experienced by crash test dummies representing humans. It has been recorded that the rate of reduction in the casualties has decreased in the last 6 years, suggesting that passive safety, which has been the main vehicle design method of casualty reduction, has reached its limits. This suggests there is a need for new active and autonomous driving technologies to reach the EU safety target to reduce road deaths to almost zero by 2050 ("Vision Zero") [2] [3].

Advanced driver assistance systems (ADAS) like adaptive cruise control, lane departure warning (LDW) or automatic emergency braking systems (AEB) have been introduced aiming to support reaching this EU target and help the driver in terms of comfort and safety, by taking over routine manoeuvres as well as reducing human errors. According to Leohold [4], human error is the primary cause of 95% of all fatal motor vehicle crashes. This conclusion shows the potential of automated driving systems to reduce further the number of fatalities and seriously injured vehicle occupants in the future. On the other hand, it can be questioned whether today's methods, safety protocols and regulations for restraint system development, primarily developed based on real accidents caused by human errors, are effective for future crash scenarios [5] [6].

SAE Level 5 automated driving scenarios (L5) [7] are characterized by higher design freedom of the vehicle interior and may arrive in the market after 2030 [8]. So-called living room or social

arrangements, where the occupants are sitting face to face in the vehicle, are expected to be common instances for future Level 5 automated vehicles [9] [10] [11] [12]. Car manufacturers might consider developing such vehicle layouts and, at the same time, have to ensure the protection of all occupants in any alternative planned seating position within the operational design domain of the vehicle. Today's methods, safety protocols and regulations for restraint system development will not be effective in such future crash scenarios because they require occupants to face forward in the vehicle cabin, as in the current crash safety standard, e.g. UNECE R94, UNECE R95. Furthermore, flexible seating arrangements with a wide range of seat positions and rotations would require new restraint system concepts [13]. This finding is an obvious consideration when looking into Level 5 automated driving, as suggested in the in-crash studies from Kitagawa et al. [11] and Zhao et al. [14]. These studies highlighted several potential higher injury risk scenarios and critical occupant motions when being oriented away from the 0° relative to the impact direction. It is presumed that to allow the seat to rotate, a (motorised pre-tensioner) seat belt, integrated into the seat structure, will be an essential part of future restraint systems [11].

Dynamic Out-of-Position (OoP) kinematics, resulting from pre-crash manoeuvres and different occupant awareness levels are not considered in the reviewed studies, but maybe required in the future [15] [16] [17]. Battaglia et al. [17], suggests to develop acceptance corridors, for example based on head trajectories. This demand is also underlined by Kitagawa et al. [11] who noted that in detectable crashes, pre-collision manoeuvres due to activation of AEB and automated emergency steering (AES), may change occupant's posture that may affect the impact kinematics. Therefore, capturing the occupant's kinematics as a function of seating position is an urgent need.

Knowing the occupant's position in an automated driving scenario during pre-braking phase will be a first step to define the requirements of future restraint systems. This paper aims to define clearance zones based on the kinematics envelope. Such clearance zones are needed to allow restraint system manufactures to develop new airbag system technology, ensuring that the occupant is anytime out of the airbag deployment zone. Additionally, they will enable the development of new vehicle interior layouts aiming to avoid undesirable occupant to occupant or occupant to vehicle contact.

The objectives of the current work are therefore to a) investigate occupant kinematics in rotated seat arrangements during a pre-crash manoeuvre using the Simcenter Madymo Active Human Model (AHM) b) define kinematics envelope for the head in the selected pre-crash manoeuvre and c) identify potential impact towards the development of supplementary safety systems like airbags.

2 Methods

The aim of this paper is to define occupant's head kinematics envelope during the pre-crash phase in expected automated level 5 driving scenarios [7]. To calculate the occupant's motion, the Simcenter Madymo AHM Version 3 is chosen because of its capability to calculate and predict the kinematics with a relative degree of confidence [18]. Also, compared to the finite element solutions, Simcenter Madymo's multi-body modelling approach requires less computational time [19]. A methodology to extract the head kinematics envelope is proposed in the following four steps and illustrated in **Figure 1**:

1. Definition of occupants' target kinematic response corridors based on controlled frontal and swerving manoeuvres, using OM4IS test data: The kinematics of 50th percentile occupants' corridors will be extracted using the method proposed by Bastien et al. [20]. This aims to capture an average behaviour of occupants in tensed and relaxed muscle activation mode in a lap-belted environment.

2. Compare the standard response of the Simcenter Madymo Active Human Model (AHM) with the extracted OM4IS corridors as explained in step 1 and calibrate the AHM parameters based on these results in order to improve its response.
3. Validate the newly calibrated Simcenter Madymo AHM obtained in step 2 against UMTRI data, which include a wider range of 3-point belted tests whilst including a more representative range of population (BMI, anthropometry, age etc...).
4. Investigate Rotated Seat Arrangements: Investigate the pre-crash kinematics of occupants in rotated seating arrangements using the validated AHM to define the “safe” envelope for occupants’ head excursion.

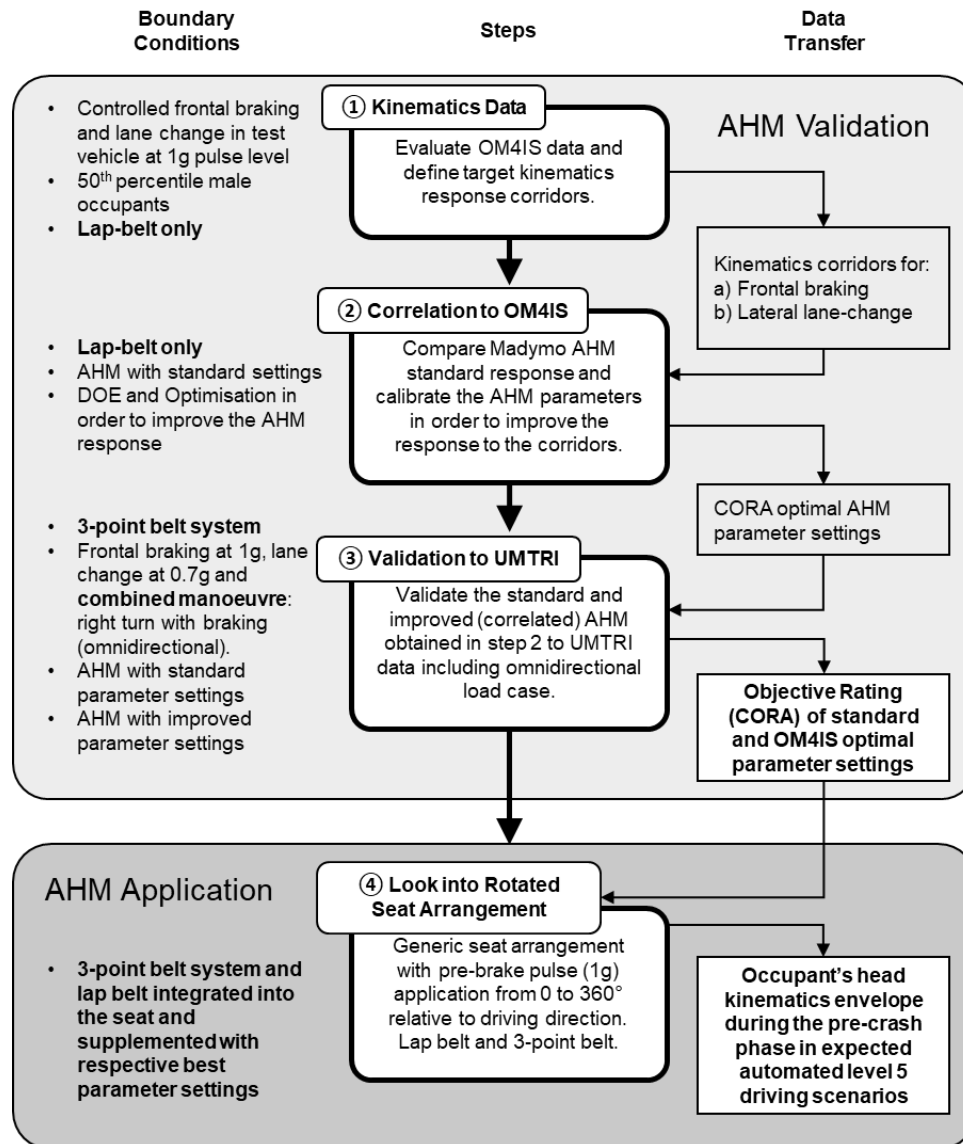


Figure 1. Methodological Workflow

These steps are chosen based on the recommendation made by Wismans et al. [3], who stated that in order to validate a computer model, it is necessary to test it against different databases, i.e. OM4IS (step 2) vs UMTRI (step 3). The model outputs are assessed in terms of forecasting ability and quality, e.g. by using the objective rating method CORA [21], which is an accepted correlation method. The AHM

validation will be covered in Section 3 of this paper, which its application in a rotated seat arrangement will be addressed in section 4.

2.1 OM4IS Occupants Kinematics' Evaluation

A deliverable of the OM4IS project was to perform full vehicle tests to investigate occupant kinematics in two common evasive manoeuvres: a) an emergency braking manoeuvre with an initial speed of approximately 10km/h at a level of 1g longitudinal deceleration and b) a lane-change manoeuvre in the style of a ISO 3888-2 single lane-change at 50km/h at a level of 1g lateral acceleration [22]. Both manoeuvres were performed with 22 male volunteers, representing the weight and size of a 50th percentile human male (weight = 77.4 ± 6.7 kg and height = 179.3 ± 4.3 cm). The manoeuvres were carried out in a defined order, aiming to investigate different awareness state of the occupants, namely uninformed, aware and informed. In total, 55 valid tests are available for the frontal braking load case and 54 for the lane-change load case respectively. All volunteers were seated on a rigid reference seat consisting of two wooden plates fixed on a Mercedes-Benz S-Class test vehicle, covered with artificial leather, making the coefficient of friction realistic. Furthermore, the occupants were restrained by a lap-belt of fixed length. The volunteers' motion data was collected by a VICON optical motion tracking system, which uses optical sensors to track marker motions in the 3-dimensional space, with the purpose to calculate the real occupants' kinematics envelope.

Similar to Huber et al. [23], the body regions were split into two segments, head and torso, which have been considered non-deformable. To capture volunteers' motion, two segments are formed: the head segment marked orange and torso segment marked green, as illustrated in **Figure 2** for pre-braking and in **Figure 3** for lane-change respectively.

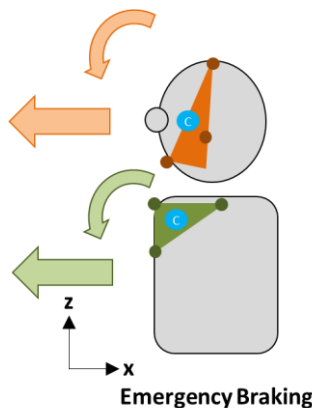


Figure 2. Occupant Motion in Pre-Braking Scenario (side view on the occupant)

Head and torso segment (grey areas) motion along vehicle x-axis and rotation about vehicle y-axis. Head segment marked orange and torso segment marked green with their respective centre point.

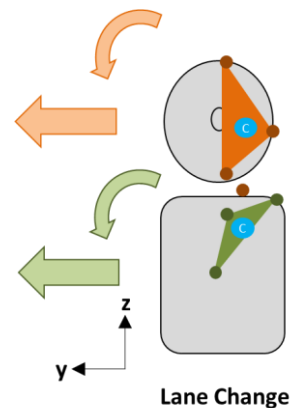


Figure 3. Occupant Motion in Lane-Change Scenario (front view on the occupant)

Head and torso segment (grey areas) motion along vehicle y-axis and rotation about vehicle x-axis. Head segment marked orange and torso segment marked green with their respective centre point.

For each of these segments, three points are chosen to define the respective quasi-rigid segment body. For the head segment these points are the top of the head, chin and left cheek and for the torso segment the left clavicle, and front and left shoulders. During an emergency pre-braking manoeuvre, the specific, or dominant motion of the occupants' body segments' motion is a combination of translation along the vehicle x-axis and rotation about the vehicle y-axis as illustrated in **Figure 2**. In the lane-change scenario, the dominant motion of the occupants' body segments is a translation along the vehicle y-axis combined with a rotation about the vehicle x-axis, as can be observed in **Figure 3**. The motion and

rotation of the orbital centre of the triangle formed by the respective three marker points is then calculated for each segment in each load case, for each volunteer in each dominant direction.

The method to define the kinematics corridors as proposed by Bastien et al. [20] starts with forming the median of the available response curves. To capture the spread of human reactions, the standard deviation (σ) is proposed to consider when forming the kinematics target curves. Applying statistics to the calculated motion and rotation data allows the computation of the median curve and a standard deviation σ for each channel of interest. Doing so allows to plot five kinematics target curves ranging from a very slow reaction (-2σ) to slow reaction (-1σ) over normal reaction (median) to fast ($+1\sigma$) and very fast reaction ($+2\sigma$). The so derived kinematics corridors are then used to correlate the Simcenter Madymo AHM.

2.2 Correlation of the Simcenter Madymo AHM to the OM4IS data

This section aims to verify the kinematics response of the Simcenter Madymo AHM Version 3.0, as of May 2018 [18], in comparison to the kinematics corridors derived in Section 2.1. For this, the response of the AHM is correlated against the OM4IS test responses, in both frontal and swerving test cases. The objective rating method CORA is used to evaluate the results by comparing the mean value of each channel for both frontal pre-braking and lateral lane-change test scenarios. In total eight channels are weighted equally and $\pm 1\sigma$ and $\pm 2\sigma$ curves are considered as inner and other corridors.

As this research looks into the pre-crash kinematics in expected Level 5 automated driving scenarios, it is important to consider rotation of the seat to cater for future occupant protection needs [9] [11] [13][14] [24]. However, unfortunately, physical test data with volunteers in rotated seats is not available. Consequently, it is proposed to use the available frontal and lateral tests to obtain the best AHM parameters to replicate both frontal and lateral occupants' responses. This is based on the assumption that these parameters will represent a realistic omnidirectional response when the seat is rotated. Therefore, the final goal is to find a parameter set which provides a CORA optimised result considering combined load cases, i.e. performing a multi-objective study aiming to receive an omnidirectional correlated model.

The AHM is placed into a vehicle environment adapted to the major parameters of the OM4IS test vehicle and restrained by a lap-belt. The marker points considered in the data evaluation are applied to the model so that the AHM's motion tracking system can relate to the same motion tracker positions used in the OM4IS tests (volunteers), as described in Section 2.1 and illustrated in **Figure 2** for pre-braking and in **Figure 3** for lane-change respectively.

The AHM parameters, which can be customised by the user and considered in this paper, are given in **Table 1**. Neural delay is hard-coded for this study, i.e. the time delay after which muscles respond to a stimulus is the sum of the reaction time parameter values. The neural delays considered are 40ms for the neck, 70ms for the spine and arms and 100ms for the legs [18]. Muscle force level, so to say the strength of the occupant, can be scaled for the neck, the arms and the legs, aiming to consider human response variations.

According to Siemens Industry Software and Services B.V. (SISS) [18], the Simcenter Madymo AHM Version 3.0 model is validated to a large number of tests addressing both model capabilities, passive and active human behaviour. By deactivating the muscle activity, the model can be used as passive HBM, for example in crash simulation, however it has never been tested against occupants wearing a lap-belt only, which is a possible scenario in future L5 vehicle cabin design environments.

Table 1. Simcenter Madymo Active Human Model (AHM) Parameters.

Parameters which can be edited by the user in the AHM model include file. The baseline settings represent the delivery state of the AHM, they represent according to SISS [18] an average 50th percentile male. The DOE range is defined in cooperation with SISS.

		Description	Value / Range	Baseline	DOE Range
Activation	Neck	Neck Muscle Activation	0 → passive behaviour > 0 → active behaviour	1.0	0.5-3.0
	Spine	Spine Muscle Activation			
	Shoulder	Shoulder Muscle Activation			
	Elbow	Elbow Muscle Activation			
	Hip	Hip Muscle Activation			
	Knee	Knee Muscle Activation			
Head Orientation	Head	Attempt for the neck controller to control the head orientation	0 → head upright (horizontal to reference space) following vestibular system (typical for occupants)	0	0 or 1
			1 → head aligned with the T1 vertebra orientation (straight neck, typical for pedestrians)		
Awareness	Neck_CCR	Isometric pre-tension of the neck muscles (co-contraction) as a reaction to danger (bracing)	[0.05 – 0.2] → relaxed [0.4 – 0.6] → braced	0.3	0.05 – 0.6
	Reaction Time	Time delay after which muscles respond to stimulus	[0 – 25ms] → reaction time of a person aware of the upcoming stimulus [60 – 160ms] → reaction time of a person unaware of the upcoming stimulus	20ms	0.0 – 160ms
Strength	Global	Strength scale factor that applies to all muscles in the model	Strength for average male	1.0	0.5 – 3.0
	Neck	Strength scale factor for neck muscle only	↑	1.0	↑
	Arms	Strength scale factor for arm muscle only	↑	1.0	↑
	Legs	Strength scale factor for legs muscles only	↑	1.0	↑

An automated analysis process has been developed to consider frontal pre-braking, lateral lane-change and both scenarios at the same time, aiming to calculate the models CORA rating depending on the AHM parameters in an automated manner. A Design of Experiment (DOE) has been designed using a Latin-Hypercube approach and consists of 100 runs to screen the models' parameters influence on the CORA rating. The modeFRONTIER (ESTECO SpA, Trieste, Italy) optimisation algorithm piOPT has been used to optimise the CORA rating aiming to find the optimal AHM parameters. The time duration (period) for the CORA rating has been set to be between 0.0s – 0.7s for the emergency braking and 0.0s – 1.3s for the lane change scenario. These time domains capture the frontal and lateral motion until the occupant reaches its initial position again. This part of the study will define the master activation parameters, which will then be validated against another dataset, here a data set from UMTRI, which has a different population demographics and a different seatbelt arrangement.

2.3 Validation of the Simcenter Madymo AHM to UMTRI data

The UMTRI tests [25] differ from the OM4IS tests in some important aspects. On one hand, a larger number of volunteers were tested in the UMTRI study and on the other hand, the test setup and test

execution were more realistic, e.g. a suit with position markers like in the OM4IS tests was not used. In addition, the occupants in the UMTRI study were told that the study performed was to assess the vehicle ride and handling and not their kinematics response. Both factors may have influenced the awareness state and therefore the results of the participants of the OM4IS study. In the OM4IS tests, only young strong men of 50th percentile stature were included, whereas the UMTRI test considers both men and women of different statures, covering a broad range of occupant groups. In total 87 adults, of which 44 are women and 43 are men participated. Their age range was 18 to 70 years with a mean of 45 years and the participants BMI range was 19 to 67kg/m² with a mean of 29kg/m². Both mean values are similar to the mean of the population of the United States.

The volunteers were placed in a standard vehicle (2016 Toyota Avalon) equipped with a standard vehicle seat. Probably the most important difference is that in the UMTRI tests a standard 3-point belt was fitted while in the OM4IS tests only a lap-belt was used. The motion of the occupants' head was tracked using a novel system based on a Microsoft Kinect Version 2 sensor.

Similar to the OM4IS test, the UMTRI tests were conducted at a higher initial velocity and longer braking duration. A full braking starting from 56km/h (peak deceleration 1g) and a lane-change with a lateral peak acceleration of 0.7g were performed. In addition, a combined scenario, right turn with braking, was conducted, which is particularly an important scenario because it is the desired omnidirectional load case that can be used to demonstrate the predictive capability of the AHM computer model.

The Simcenter Madymo AHM is placed in a vehicle environment comparable to the UMTRI test vehicle and restrained by a 3-point seat belt. Beside others, Reed et al. [25] limited their findings to the seat design and the presence of the centre console. Specifically, the latter may have influenced occupant lateral excursions in the lane-change and right turn with braking load cases. It has indeed been observed from the video evaluation that nearly all participants' torsos and elbows were contacting the centre console. To evaluate this effect and thus the sensitivity of lateral torso guidance, a second model was studied where the centre console width has been reduced by 40mm and therefore the gap between the occupant and the console increased by 20mm.

Reed et al. positioned the head COG kinematics data of all participants into one dataset and provided the mean and $\pm 1\sigma$ which is very similar to the proposal of Bastien et al. [20]. The $\pm 2\sigma$ data was calculated and both are considered in the CORA rating similarly to the approach given in Section 2.2. The AHM is then simulated in the considered scenarios using the found optimal parameter set from the OM4IS correlation and its standard settings for comparison. Both parameter sets can be observed in **Table 2**.

2.4 Rotated Seat Arrangements

In order to extract the pre-crash kinematics' envelope and to define the enclosed occupants' motion volume space, the validated Simcenter Madymo AHM is placed into a possible future automated vehicle seat arrangement.

Figure 5 illustrates the AHM seated in the seat supplemented with a standard 3-point seat belt system while **Figure 6** illustrates the second scenario with a lap belt only. In reference with the work of Kitagawa et al. [11] and Jorlöv et al. [9], the seat arrangement is modelled in such a way that it can be turned with respect to the driving direction around the vehicle z-axis by 360 degrees.

While the seat is fixed in space for all scenarios, the driving direction and therefore the seat direction with respect to the applied pre-brake pulse is changed. The simulations are conducted for a variable angle ϕ_z , varied between 0 and 360° in steps of 22.5°. The red arrow, illustrated in **Figure 4**, indicates

the driving direction and the direction of the applied generic 1g pre-brake pulse which as can be observed in **Figure 7** for $\phi_z=0$. The pre-crash pulse rises within 0.3s from $t=0$ s to the maximum of 1g which is then kept constant until the end of the simulation at $t=2.0$ s. The pulse is comparable to the one found in the OM4IS data and presented by Reed et al. [25].

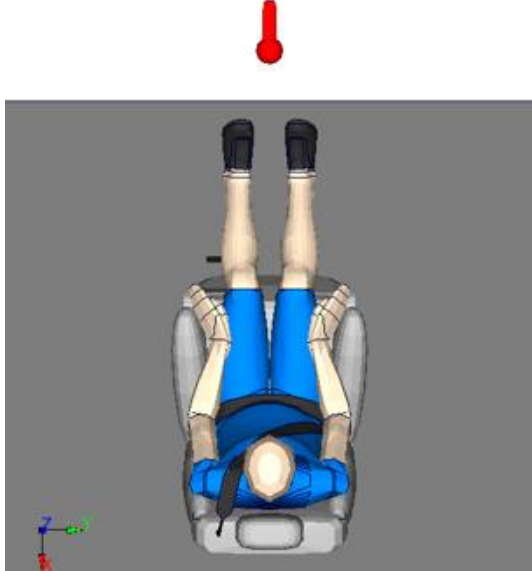


Figure 4. Rotated Seat Arrangement, Top View
red arrow indicating driving direction and direction of pulse application (0-360°).



Figure 5. Isometric View with 3-point seat belt



Figure 6. Isometric View with lap-belt

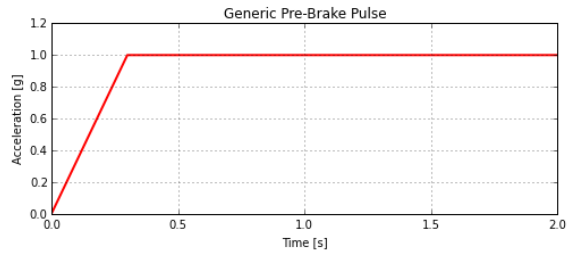


Figure 7. Generic 1-g Pre-Brake Pulse
Rise to 1g within 0.3s

The Simcenter Madymo baseline seat model is a standard seat model provided by SISS that is used in industry for concept design because of its realistic shape, dimensions and cushion stiffness [26]. The seat back angle is set to 20°. Additionally, the seat belt system, in particular the upper D-Ring position, is fixed to the seat instead of the vehicles' B-pillar, which is a prerequisite to allow the turning of the seat relative to the vehicle structure.

The AHM head COG motions in the xy-plane are evaluated to form the kinematics' envelop and to define the enclosed movement space in that plane. To consider the human variance, the corridors proposed by Reed et al. [25] are used. In Reed's study, it was observed that the $\pm 1\sigma$ corridors could be described as a percentage of the mean value to be (on average) $\pm 48\%$ for frontal motion and $\pm 28\%$ for lateral motion. The results of the AHM are considered to represent this dispersion in Section 3.4.

3 Results of the AHM Validation

This section will present the results of the AHM validation in accordance to the three validation steps defined in the methodology.

3.1 OM4IS Occupants Kinematics' Evaluation

The resulting five kinematics target curves for the occupants' dominant motion during the respective driving manoeuvres can be observed in Appendix A. The median reaction curves are drawn in solid black, the $\pm 1\sigma$ corridors in dark grey and the $\pm 2\sigma$ corridors in light grey respectively. The AHM overlay response will be presented in Section 3.2.

3.2 Correlation of the Simcenter Madymo AHM to the OM4IS data

This section provides the results of the combined DOE and the subsequent optimisation and thus the CORA optimal master AHM parameter settings for the validation to the UMTRI data. All 100 DOE and 38 successive optimisation simulation leading to a total of 276 simulations.

A wide spread of CORA rating score was observed in the DOE: 0.47 to 0.79, which corresponds to a fair and good rating according to ISO/TR 9790 respectively. A Smoothing Spline Analysis of Variance (SS-ANOVA) was carried out for the objective function. The two parameters, **ReactionTime** (52.2%) and **SpineActivation** (31.2%) where the main contributors to the CORA score variance, accounting together for 83.4% of its variance. The baseline parameter settings result in a total CORA score of 0.64 (fair). The overlay of the baseline AHM results to the correlation corridors is illustrated in **Figure 8** and **Figure 9** for emergency braking and lane-change (solid blue) scenarios respectively.

The CORA score for the optimal design parameters found is 0.79 (good). The overlay of the AHMs kinematic response is illustrated in **Figure 8** for emergency braking and in **Figure 9** for lane-change (solid red). A significant improvement can be noticed in comparison to the baseline parameter set results. The parameters **NeckActivation**, **HipActivation** and **KneeActivation** tend towards the lower boundary of their respective parameter space. In contrast, the parameters **SpineActivation**, **ShoulderActivation**, **ElbowActivation** and **Neck_CCR** tend towards their upper boundary. The value for parameter **HeadRef** is found to be 0, indicating the head alignment to be horizontal, which is in general typical for occupants [18]. **Table 2** provides an overview of the rating results and the master parameters computed in the optimisation.

Table 2. Results of the Correlation to OM4IS data set.

Simcenter Madymo AHM Parameters, CORA Score and ISO/TR 9790 rating for the combined correlation to the OM4IS data set, considering emergency braking and lane-change at the same time.

		Baseline	CORA Optimal
Activation	Neck	1.0	0.5
	Spine	↑	3.0
	Shoulder	↑	3.0
	Elbow	↑	3.0
	Hip	↑	0.5
	Knee	↑	0.5
Head Orientation	Head	0	0
Awareness	Neck_CCR	0.3	0.6
	Reaction Time	20ms	0.0ms
Strength	Global	1.0	2.86
	Neck	↑	↑
	Arms	↑	↑
	Legs	↑	↑
CORA Score		0.64	0.79
ISO/TR 9790		fair	good

The visual kinematics comparison in the emergency braking scenario with the response of a median volunteer confirms the findings obtained in the objective rating for the CORA optimal design. As can be observed in **Figure 31** (Appendix B), the kinematics of the AHM computer model, whose parameters are set as shown in **Table 2** (CORA Optimal), predict well the motion of the median occupant during the time frame considered for the CORA rating (0 – 0.7s). The striving of the AHM to come back to its initial position is compared to the test not so pronounced for the time period $t > 0.7s$. Comparing the final head position to the median volunteer indicates that the head rotates more backwards, which is also seen in the curve overlay, **Figure 8** (bottom left).

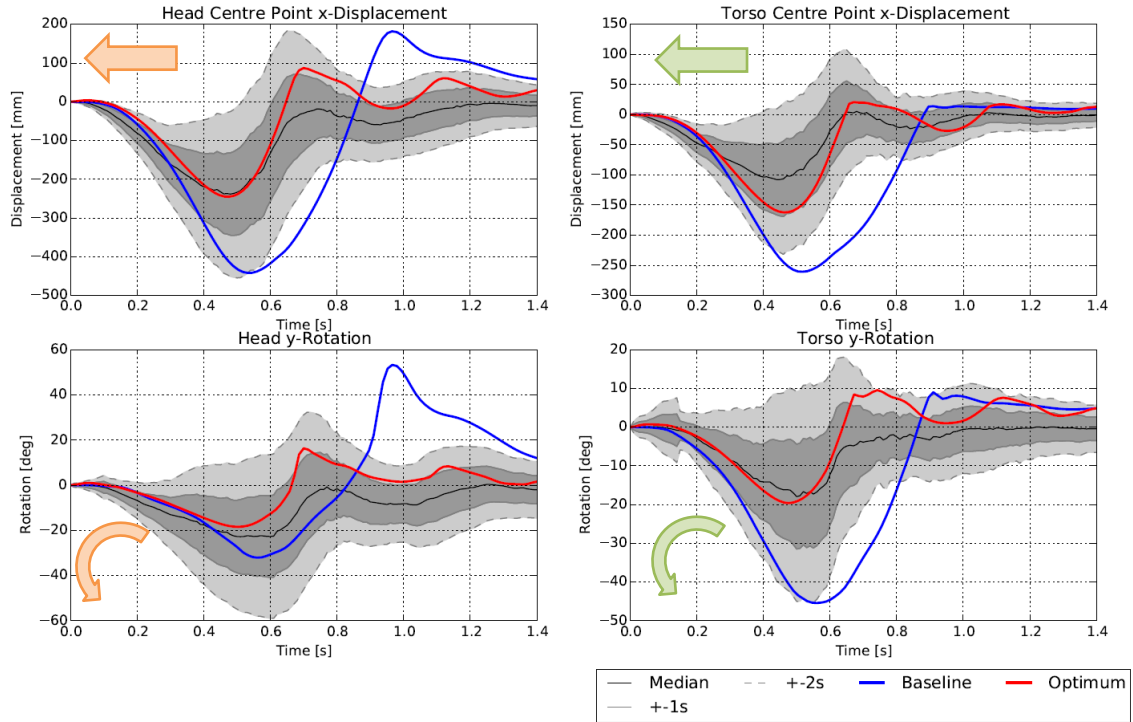


Figure 8. Overlay of the Results for OM4IS Emergency Braking over the Corridors.
The results for the baseline parameter settings are drawn in blue and the results for the found optimal master settings are drawn in red. Top left: head centre point x-displacement, top right: torso centre point x-displacement, bottom left: head centre point y-rotation and bottom right: torso centre point y-rotation.

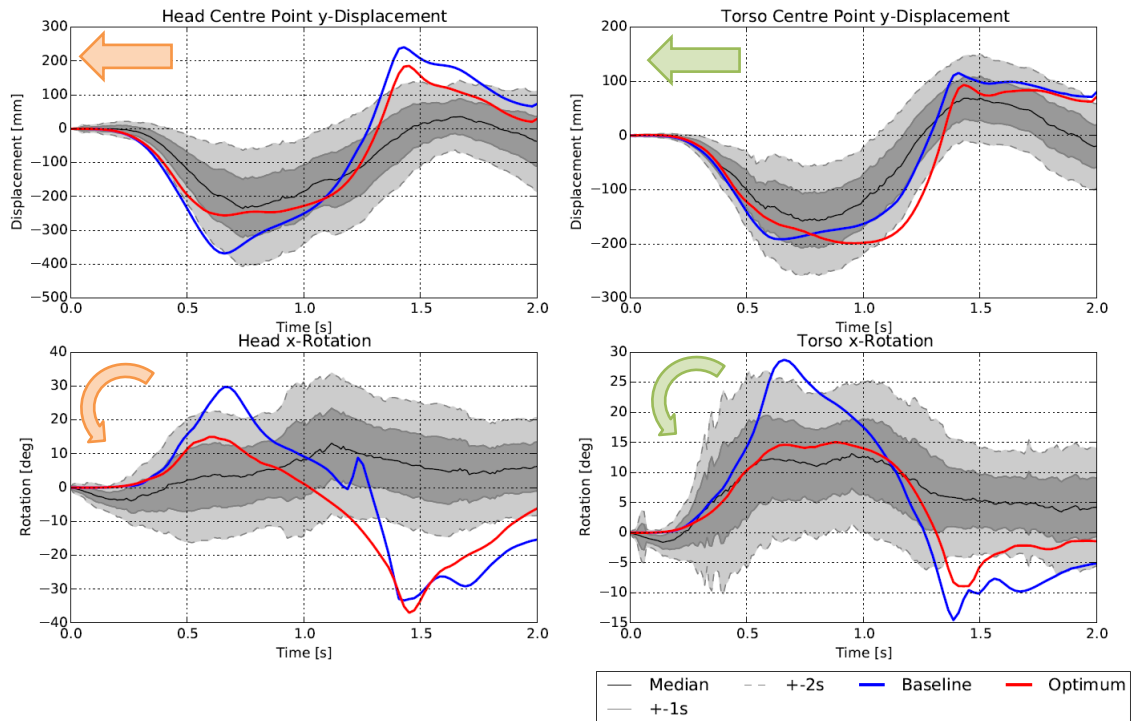


Figure 9. Overlay of the Results for OM4IS Lane-Change over the Corridors.
The results for the baseline parameter settings are drawn in blue and the results for the found optimal master settings are drawn in red. Top left: head centre point y-displacement, top right: torso centre point y-displacement, bottom left: head centre point x-rotation and bottom right: torso centre point x-rotation.

In principle, the results for the lane-change are similar to the ones of the emergency braking. However, the head rotation of the AHM is more pronounced in comparison to the test at the time of the maximum lateral displacement towards the vehicle centre ($t = 0.8\text{s}$), which is observed in the data shown in **Figure 9** (bottom left) and in **Figure 32** (Appendix C). In **Figure 9** and **Figure 32**, the master model's behaviour is comparable to the volunteers' kinematics and shows at $t = 1.5\text{s}$ a maximum head position close to the door window whereas the median occupant is close to its initial position. Because of the greater head excursion towards the window, the AHM is not stabilised to the initial position at the end of the simulation run.

In conclusion, it can be suggested that in a lap-belt configuration the new activation parameters have improved the occupant's kinematic predictions over the AHM software vendor's standard settings from 0.64 (fair) to 0.79 (good).

3.3 Validation of the Simcenter Madymo AHM to UMTRI data

This section aims to validate the AHM standard parameter setting and the CORA optimal master parameters obtained against the UMTRI data set. A universal AHMs active parameter set is proposed, which will be used in the application of the AHM within the possible future seat arrangement described in Section 2.4.

From **Figure 10**, it can be noted that for the braking event, the OM4IS optimal AHM appears stiffer than the average response in the UMTRI tests. In particular, the head COG maximum frontal motion is approximately 65mm less than the median of the validation data set (drawn in black, $\pm 1\sigma$ corridor in grey). However, the overall shape, phase and amplitude of the OM4IS optimal AHMs' head COG motion shows a good correlation with the corridor proposed by Reed et al. [25]. The baseline AHM behaves softer as the OM4IS optimal and its head COG excursion is in the range of the mean in the time frame between $t = 0.25\text{s}$ and 1.0s . After $t = 1.0\text{s}$, the AHM moves backwards and deviates from the median with a steeper slope than the OM4IS optimal one.

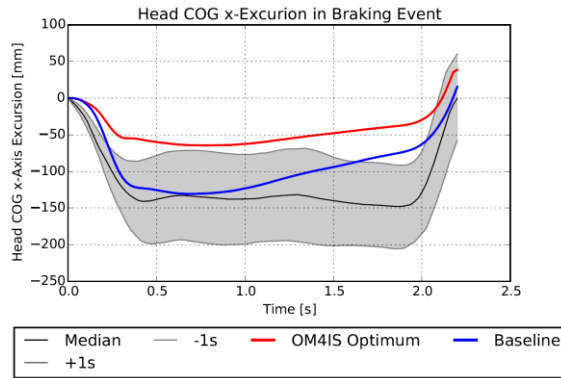


Figure 10. Result of the head COG x-excursion of the UMTRI braking event validation.
The baseline parameter settings are drawn in blue and the CORA optimal master parameters in red.

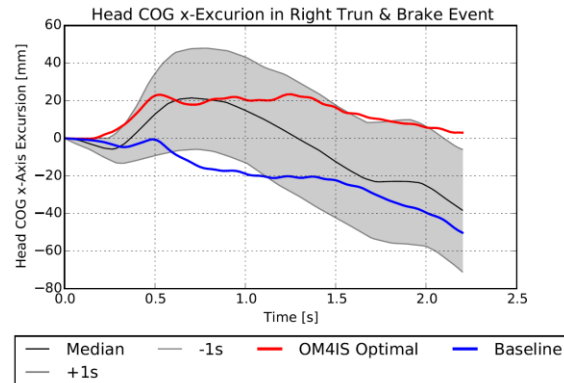


Figure 11. Results of the head COG x-excursion of the right turn and brake event.
The baseline parameter settings are drawn in blue and the CORA optimal master parameters in red.

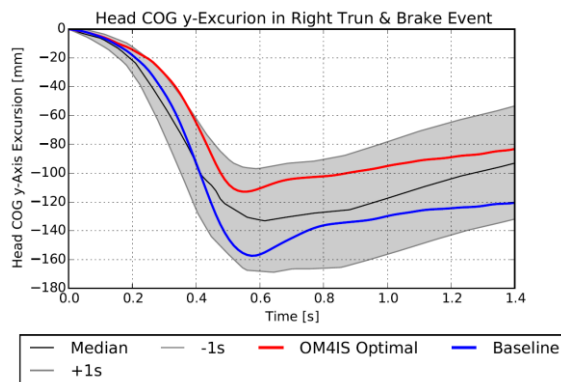


Figure 12. Results of the head COG y-excursions of the right turn and brake event.
The baseline parameter settings are drawn in blue and the CORA optimal master parameters in red.

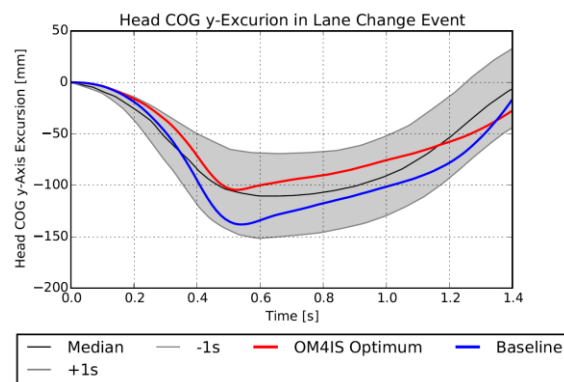


Figure 13. Results of the head COG y-excursion of the lane-change event.
The baseline parameter settings are drawn in blue and the CORA optimal master parameters in red.

The visual comparison of the OM4IS optimal AHM kinematics to a participant given in the report of Reed et al. is illustrated in Appendix D (**Figure 33**) and it can be observed that the model response correlates well with the participants' responses.

In the right turn with braking event, it is found that the Simcenter Madymo AHM with the OM4IS optimal parameters appears similar in the x-direction (frontal) compared to the mean of the data set, as illustrated in **Figure 11**. In particular, the head COG maximum frontal motion is approximately 20mm, similar to the median. This motion remains throughout the scenario and leads to the fact that the OM4IS optimal AHMs' head COG x-motion deviates from the median for $t > 1.0s$. However, the overall shape, phase and amplitude of the OM4IS optimal AHMs' head COG motion, shows a good correlation with the corridor and, especially for the time $t < 1.0s$, a more realistic corridor fit than the baseline AHM. In **Figure 12**, it can be noted that both parameter settings match the test corridor well throughout the time span considered.

Illustrated in **Figure 13**, the OM4IS optimal Simcenter Madymo AHM behaves in a similar manner compared to the mean curve of the UMTRI tests. In particular, the head COG maximum lateral motion, which is approximately same as the median for the time interval $t = 0$ to $1.0s$. The baseline AHM behaves softer, which can be observed by a higher lateral excursion at $t = 0.5s$. However, the overall shape, phase and amplitude of both AHM parameter sets, shows a good correlation to the corridors. The visual

comparison of the OM4IS optimal AHM kinematics to a participant given in the report of Reed et al. is illustrated in Appendix D (**Figure 34**) and it can be observed that the model response correlates well to the response obtained from the participant.

As described in Section 2.3, a second model (UMTRI) was analysed to study the effect of the centre console width to lateral head excursions in the lane-change scenario. Doing so evaluates the sensitivity of the lateral torso guidance towards the head excursions. It is observed that the maximum lateral excursion of the head COG changes with a 20mm larger gap towards the centre console. In particular, the minimum excursion visible for the original (OM4IS optimal) model is -104mm, compared to -114mm for the modified model, an increase of 10mm.

It can be observed in **Table 3** that the overall CORA score for the Simcenter Madymo AHM, using the OM4IS optimal parameters given in **Table 2**, is 0.82, whereas the baseline parameter settings lead to an overall CORA score of 0.84. Although the baseline AHM is slightly improved compared to the OM4IS optimal, both scores correspond to a good evaluation according to ISO/TR 9790 for the UMTRI data set.

Table 3. CORA Rating Score Summary for the Validation of the Simcenter Madymo AHM to the UMTRI Tests

Simcenter Madymo AHM Parameters, CORA score and ISO TR/9790 rating for the combined correlation to the OM4IS data set, considering emergency braking and lane-change at the same time.

Scenario	Baseline		OM4IS Optimal	
	CORA Score	ISO/TR 9790	CORA Score	ISO/TR 9790
Braking	0.89	good	0.62	fair
Right Turn & Braking	0.76	good	0.84	good
Lane-Change	0.95	excellent	0.96	excellent
Total	0.84	good	0.82	good

The results suggest that both parameter sets for the Simcenter Madymo AHM can predict the human kinematics in a combined pre-crash scenario with a higher degree of confidence. In order to decide which parameter set to be used to investigate kinematics of occupants in rotated seat arrangements, the CORA score considering both test databases (OM4IS and UMTRI) is calculated by weighting both databases equally and presented in

Table 4. It can be observed that both, baseline and the OM4IS optimal parameter sets, show a good overall rating but the rating for the baseline settings in the lap-belted OM4IS test is only fair.

As research is ongoing also for future seat belt designs, e.g. Östling et al. [27] propose a so called criss-cross belt, it may not be presupposed that future vehicles still use today's standard 3-point seat belt. For example, modern buses use a lap-belt to restrain occupants in an event of a crash. Hence, the model applied in Section 2.4, and evaluated in Section 4, should be as much as possible independent from the parameter "belt system", which presupposes that it shows good CORA rating results in all belt system scenarios considered.

However, the fair rating for the braking scenario using the OM4IS optimal parameter set must be considered when looking into scenarios using a torso restraining seat belt device. Based on the average CORA rating scores given in

Table 4, it is therefore proposed to use the OM4IS optimal parameter settings when looking into future seat arrangements without torso restraint (lap-belt) and the Simcenter Madymo baseline parameters with torso restraint (3-point belt). The present results suggest that this provides good kinematics results with respect to the seat belt system concept.

Table 4. Simcenter Madymo AHM CORA Rating Score Summary for OM4IS and UMTRI test databases

Test Database	Baseline		OM4IS Optimal	
	CORA Score	ISO/TR 9790	CORA Score	ISO/TR 9790
OM4IS	0.64	fair	0.79	good
UMTRI	0.84	good	0.82	good
Total	0.74	good	0.81	good

4 Occupant Kinematics in Rotated Seat Arrangements

This section analyses the occupant's kinematics response as a function of seat rotation for a standard 1g frontal deceleration. The head COGs' pre-crash kinematics envelope is extracted considering a lap-belt and a standard 3-point seat belt. This allows defining the occupants' "safe" envelop. The activation parameters for the AHM have been set to Simcenter Madymo Baseline for the 3-point belt and the OM4IS optimal for the lap-belt scenario as given in **Table 2**.

4.1 3-Point Seat Belt System Kinematics

The kinematics response for the 3-point belt scenario can be divided into two Phases. Phase 1 is the movement as reaction to the 1g pre-crash pulse where the occupant just moves due to the acceleration to an approximately maximum displacement. In Phase 2 ($t > 0.4s$) the occupants endeavours to stabilize its posture against the acceleration.

Phase 1 lasts approximately until $t = 0.4s$. The occupant kinematics at $t = 0.4s$ can be observed in **Figure 14 Error! Reference source not found.** for 0° until 315° in steps of 45° seat rotation angle. **Figure 15** illustrates the head COG movement trajectory for all angles considered ($0 - 360^\circ$ in steps of 22.5°) and provides the head COG's position at $t = 0.4s$. The error bars indicate the $\pm 1\sigma$ deviation given by Reed et al. [25]. It can be observed that the 3-point seat belt seems to have a significant influence on the occupants' motion as the motions for the angles between 0° and 180° are considerably lower than the motion between 180° and 315° . For example, the amount of xy-motion for 22.5° is $x = 90mm$ and $y = 63mm$ whereas for 337.5° it is $x = 120mm$ and $y = 89mm$, as can be observed in **Figure 16**. This may be due to the fact that the 3-point seatbelt does not restrain the occupant symmetrically, rather the restraint is higher on the side where the belt is located on the shoulder, the occupants' left side in this instance. The amount of lateral motion is similar to the frontal motion.

Top View of the rotated seat arrangement at $t = 0.4\text{s}$ with 3-point seat belt system:

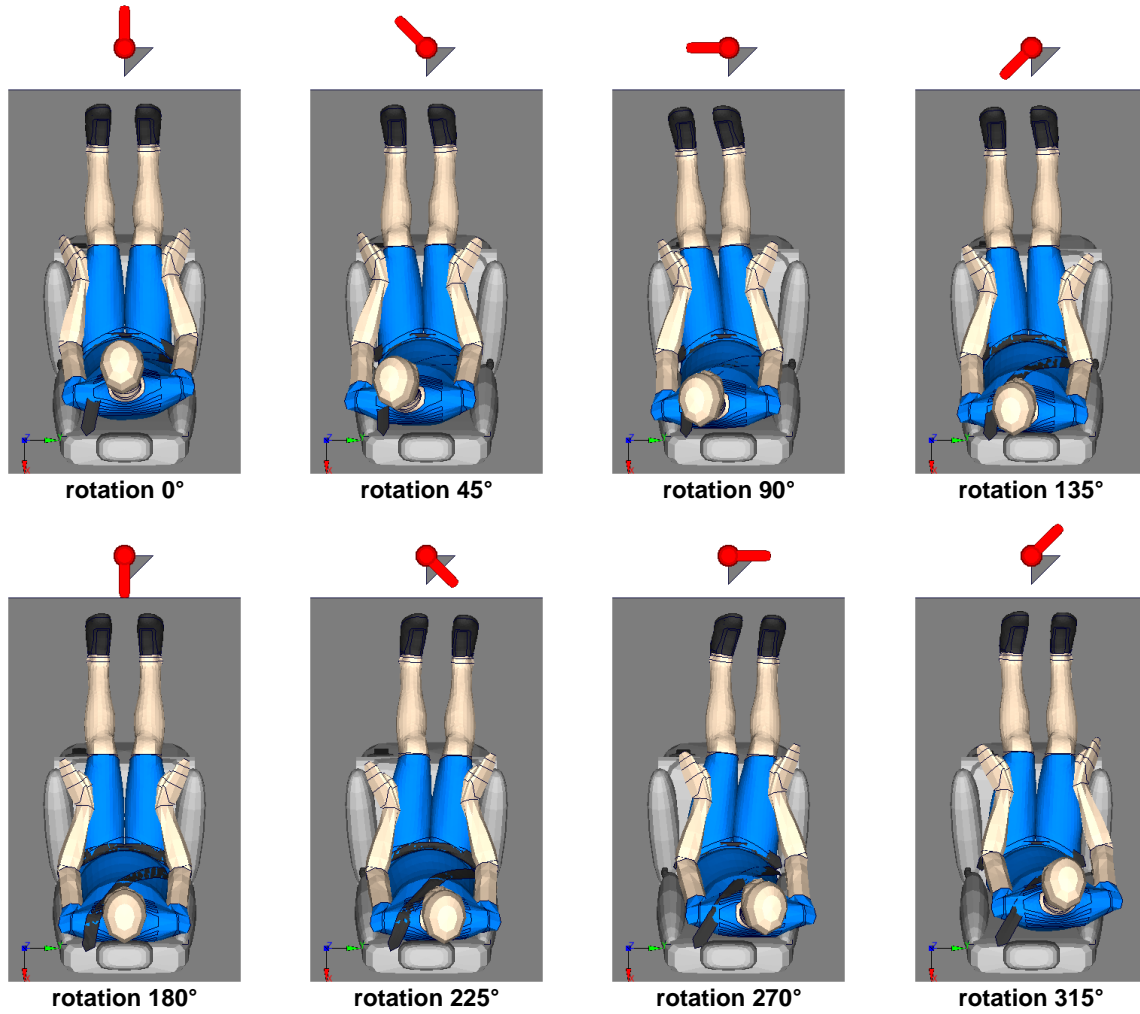


Figure 14. 3-point seat belt, rotation 0° - 315°. Top view of the rotated seat arrangement at $t = 0.4\text{s}$ where the occupant is at an approximately maximum displacement.

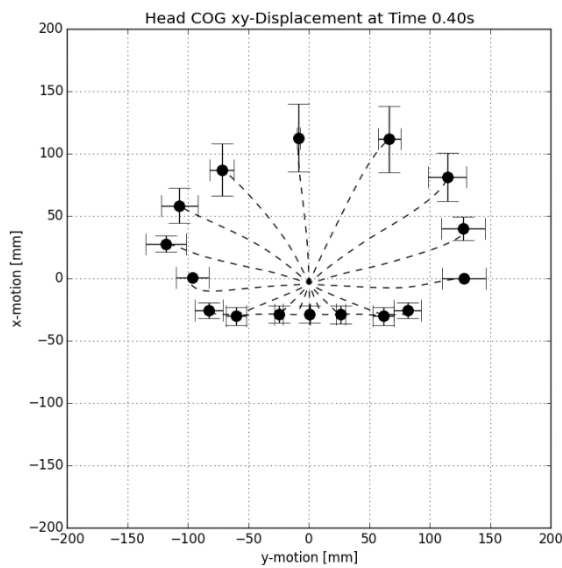


Figure 15. Head COG xy-displacement and trajectories at $t = 0.4\text{s}$ for all rotation angles considered.

The error bars indicate the $\pm 1\sigma$ deviation.

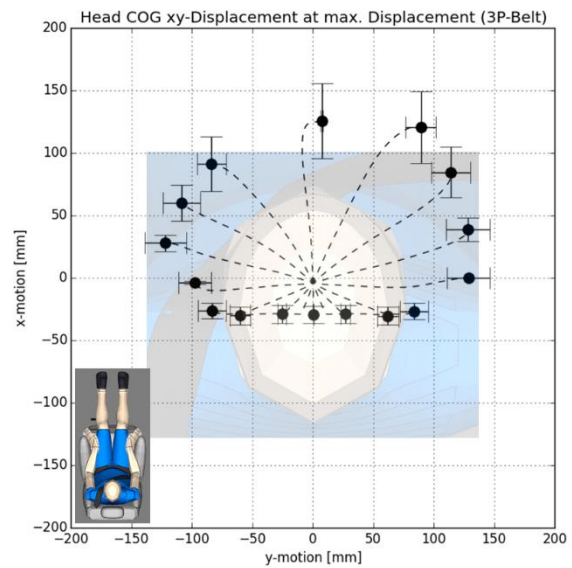


Figure 16. Head COG xy-displacement and trajectories at maximum resultant displacement for all rotation angles considered.

The error bars indicate the $\pm 1\sigma$ deviation.

Phase 2 relates to the reaction movement (reflex), the phase where occupants react to the loading by activating their muscles, which is here characterised by the circumstance that the occupant tries to stabilize especially the head. Phase 2 starts after approximately 0.4s and lasts, due to the fact that the acceleration is a constant 1g throughout the rest of the simulation, until the end of the simulation at $t = 2.0$ s. In all the scenarios considered, the occupant tends to move its head back to an upright horizontal position, which can be observed in **Figure 16** and in the time series plots in Appendix E. **Figure 16** in particular illustrates the head COG xy-displacement and trajectories at the time of individual maximum resultant displacement in the xy-plane for all rotation angles considered. The backwards return motion depends on the position of the head rest relative to the head because for angles around 180° the motion is limited when the person hits the head rest.

4.2 Lap-Belt Seat Belt System Kinematics

The kinematics response for the lap-belt scenario can, like for the 3-point belt, be divided into two Phases. Phase 1 is the reaction movement due to the 1g pre-crash pulse where the occupant just moves due to the acceleration to an approximately maximum displacement. Phase 1 lasts approximately until $t = 0.6$ s, i.e. 0.2s longer compared to the 3-point belt scenario. It has been observed that this lag was caused by the occupant's torso, which was not restrained by a belt system.

In Phase 2 ($t > 0.6$ s) the occupants' reflexes are activated to stabilize against the acceleration. The occupant kinematics at $t = 0.6$ s can be observed in **Figure 17****Error! Reference source not found.** for 0° until 315° in steps of 45° seat rotation angle. **Figure 18** illustrates the head COG movement trajectory for all angles considered ($0 - 360^\circ$ in steps of 22.5°) and gives the position of the head COG at $t = 0.6$ s. The error bars indicate the $\pm 1\sigma$ deviation given by Reed et al. [25]. Similar to the 3-point belt scenario, it can be observed that lateral motion is approximately same as the frontal motion. However, both frontal and lateral motions are approximately two times higher as with 3-point belt, which suggests that the lap-belt is not so effective like the 3-point seat belt in restraining the torso.

Phase 2 is the reaction movement, the phase where the occupant reacts to the loading, i.e. stabilization of torso and head. It starts after approximately 0.6s and lasts, due to the fact that the acceleration is a constant 1g throughout the rest of the simulation, until the end of the simulation at $t = 2.0$ s. In all scenarios considered, the person tends to move the head back to an upright horizontal position, which is highlighted in **Figure 19** and in the time series plots in Appendix F. **Figure 19** illustrates the head COG xy-displacement and trajectories at the time of individual maximum resultant displacement in the xy-plane for all rotation angles considered.

The backwards return motion depends here as well on the position of the head relative to the head rest, because for the angles around 180° the motion is limited when the person hits the head rest.

Top View of the rotated seat arrangement at $t = 0.6s$ with lap-belt seat belt system:

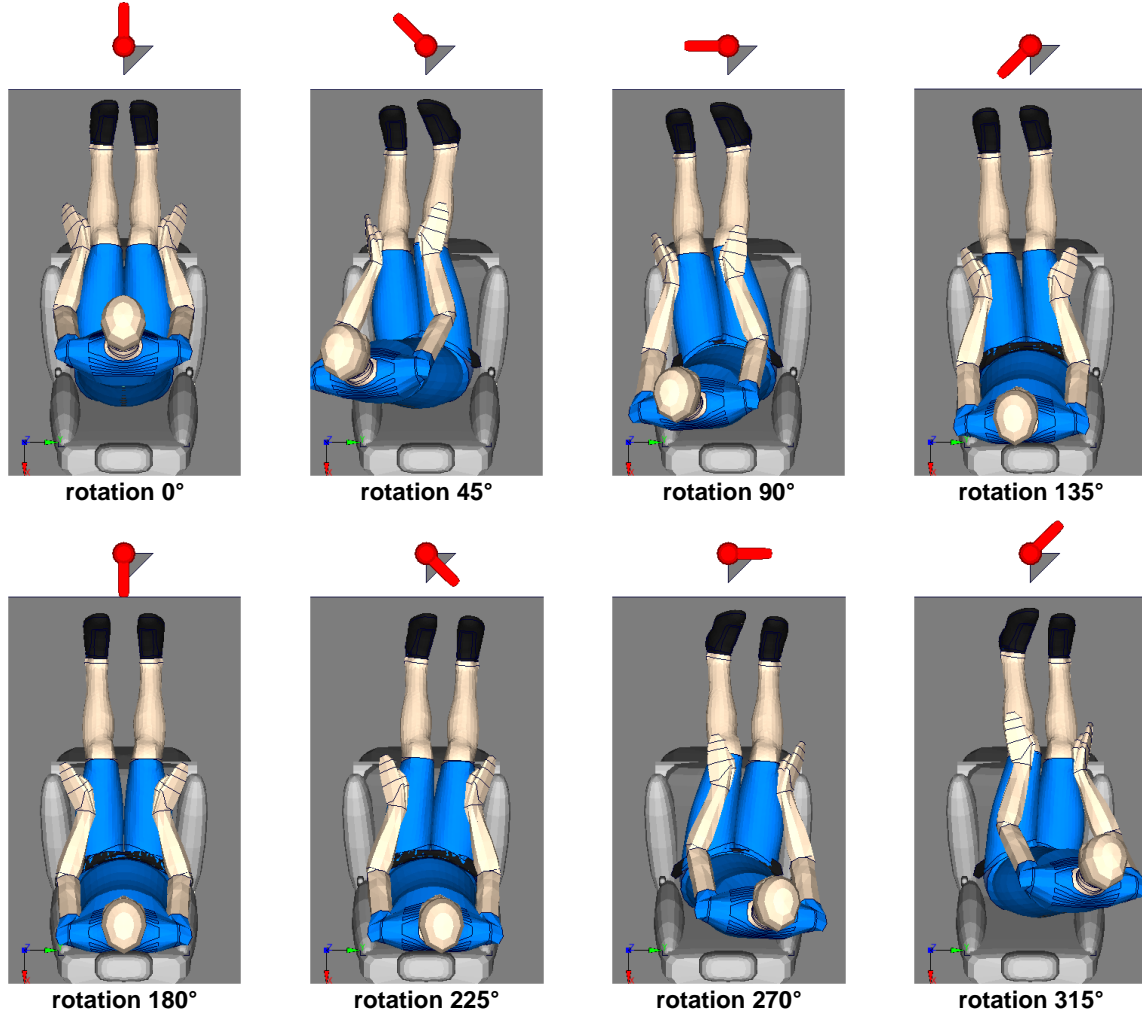


Figure 17. lap-belt seat belt, rotation 0° - 315°. Top view of the rotated seat arrangement at $t = 0.6s$ where the occupant is at an approximately maximum displacement.

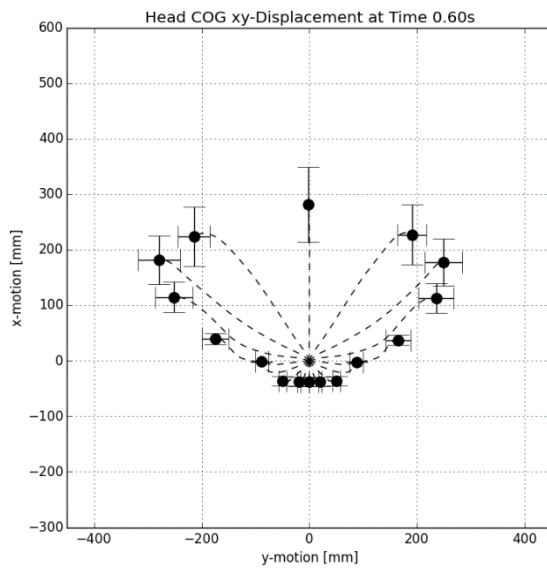


Figure 18. Head COG xy-displacement and trajectories at $t = 0.6s$ for all rotation angles considered.

The error bars indicate the $\pm 1\sigma$ deviation.

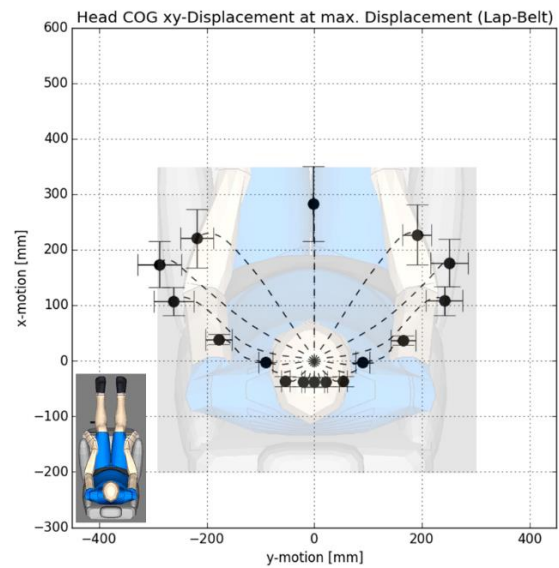


Figure 19. Head COG xy-displacement and trajectories at maximum resultant displacement for all rotation angles considered.

The error bars indicate the $\pm 1\sigma$ deviation.

4.3 The Occupants' Kinematics Envelope in an L5 Pre-Crash Phase

Following Section 4.1 and 4.2, which presented the pre-crash kinematics' envelope for the 3-point seat belt system and lap-belt system respectively, the enclosed space in which the occupant moves in a rotated seat arrangement will be investigated.

Figure 16 illustrates the head COG xy-displacement and trajectories at the time of individual maximum resultant displacement in the xy-plane for all rotation angles considered for the 3-point belt system in the rotated seat arrangement. This data serves as basis for the qualitative kinematics envelope illustrated in **Figure 20**. It is observed that in the lateral y-direction the mean occupant head COG envelope (blue curve) is within $130\text{mm} \pm 20\text{mm}$ for positive and negative y-axis. On the positive x-axis, the frontal envelope, is within $125\text{mm} \pm 25\text{mm}$ while the negative x-axis, the back envelope, is limited by the head rest at approximately 50mm. Furthermore, the finding that the 3-point seatbelt does not restrain the occupant symmetrically, reduces the kinematics' envelope on the side where the belt is present on the shoulder. In summary, it can be stated that the kinematics envelope in the investigated L5 pre-crash scenario is with regard to the lateral accelerations similar pronounced as for frontal accelerations.

Figure 19 illustrates the head COG xy-displacement and trajectories at the time of individual maximum resultant displacement in the xy-plane for all rotation angles considered for the lap-belt system in the rotated seat arrangement. This data serves as basis for the qualitative kinematics envelope illustrated in **Figure 21**. It is observed that in the lateral y-direction scenario, the mean occupant head COG envelope (red curve) is within $280\text{mm} \pm 40\text{mm}$ for positive and negative y-axis. On the positive x-axis, the frontal envelope, is within $280\text{mm} \pm 70\text{mm}$ while the negative x-axis, the back envelope, is limited by the head rest at approximately 50mm. Unlike the 3-point belt envelope, the lap-belt envelope is approximately symmetrical to the yz-plane. In summary, it can be stated that the kinematics' envelope in the investigated L5 pre-crash scenario is with regard to the lateral accelerations similar pronounced as for frontal accelerations.

The overlay of both envelopes is illustrated in **Figure 22**. The effectiveness of the 3-point belt can be observed by reducing the frontal envelop (including 1σ) for the 0-degree impact by 200mm from 350mm to 150mm, which is a reduction of 57.2%. Laterally, a similar reduction of 53.1% from 350mm to 150mm is observed.

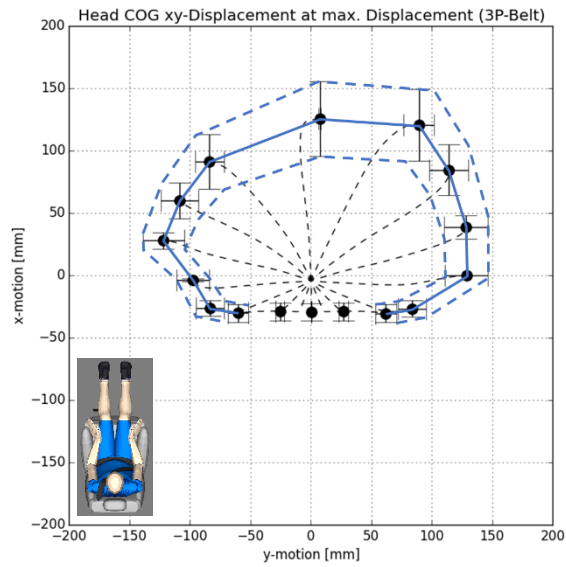


Figure 20. 3-Point Belt Kinematics Envelope in a L5 Pre-Crash Phase.

The blue line indicates the median envelope and the dotted blue lines approximately the $\pm 1\sigma$ corridors.

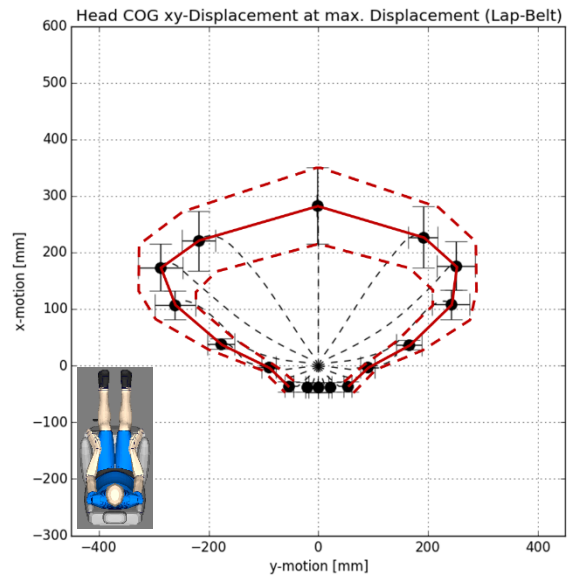


Figure 21. Lap-Belt Kinematics Envelope in a L5 Pre-Crash Phase.

The red line indicates the median envelope and the dotted red lines approximately the $\pm 1\sigma$ corridors.

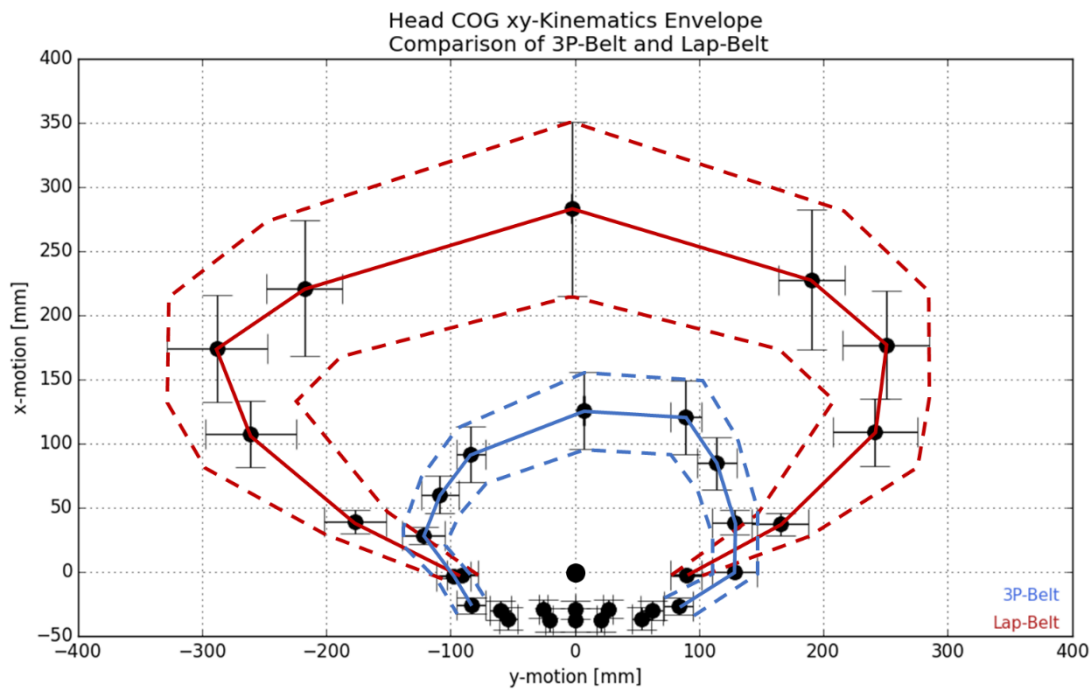


Figure 22. Head COG Kinematics Envelope for 3-Point Belt and Lap-Belt in Comparison.

The 3-point belt scenario is drawn in blue and the lap-belt scenario in red. Median solid and the dotted lines approximate the $\pm 1\sigma$ corridors.

5 Discussion

The kinematics of 50th percentile occupant corridors are extracted from the OM4IS data using the method proposed by Bastien et al. [20] and capture an average behaviour as well as tensed and relaxed, in a lap-belted environment. 55 valid tests for the emergency braking and 54 for the lane-change put the statistics on a significantly broader base compared to the 9 frontal sled tests considered in the study of Bastien et al. [20]. The derived reaction corridors, illustrated in Appendix A, can be used for validation of AHMs, considering reaction curves ranging from a very slow (-2σ) to slow (-1σ) over normal (median) to fast ($+1\sigma$) and very fast reaction ($+2\sigma$).

The successive correlation of the Simcenter Madymo AHM shows reasonable responses and suggest that in a lap-belt scenario (combined frontal and lateral load cases), the new activation parameters have improved the occupant's kinematic predictions over from the standard AHM settings. Using the CORA optimal parameters given in **Table 2**, the model scores 0.79 (good), a significant improvement from the baseline settings (0.64, fair). The visual comparison of the model results to the pre-brake event confirms that the kinematics fit well for the time period considered for the CORA rating but diverge in the later period. This conclusion is also valid for the comparison of the lane-change event. The **ReactionTime** (52.2%) and **SpineActivation** (31.2%) are the most important parameters, contributing to 83.4% of the CORA score variance.

The Reaction Time tends in all investigated scenarios to its lowest possible value of 0.0s. As neural delays are hard-coded in the AHM, there is consequently no scope for this study to consider these delays as a parameter. When trying to improve the CORA score further, it assumed beneficial to be able to modify these hard-coded neural delays to a lower value. On the other hand, humans tend to brace in pre-crash scenarios [19] [26] [27]. This can be understood as an important factor to improve the overall CORA score because the Simcenter Madymo AHM Version 3 is so far only capable to consider bracing for the neck region (**Neck_CCR**), and not for other body regions like for example the spine [26]. Potentially, the consideration of bracing may help to improve the AHMs limited trend to stabilise back to the initial position. However, it should be noted that the OM4IS volunteers were healthy young men of approximately 50th percentile stature only. Additionally, it is questioned how uninformed an occupant is, when being in a test vehicle on a closed test track and wearing a skin-tight suit. These two aspects may influence the OM4IS correlated AHMs performance when predicting “real” occupant kinematics in “real” vehicles and “real” traffic situations.

Both aspects are addressed in the successive validation of the AHM to the UMTRI test data. On one hand, a larger number of volunteers (male, female, different BMIs) were included and on the other hand, the test setup and execution were more realistic. But probably the most important difference is that in the UMTRI tests a standard 3-point belt was used and in the OM4IS tests only a lap belt. The Simcenter Madymo AHM is validated to a number of tests considering a 3-point belt and shows here a good performance and achieved a good CORA rating using the baseline factory parameter settings [18]. In the frontal braking scenario, the CORA optimal parameter settings achieved only a fair (0.62) rating while the AHM with standard parameters achieves a good (0.89) rating, as given in **Table 3**. The main reason for this is that the forward motion of the head COG is approximately 65mm less than the median (approx. 140mm) while the AHM with baseline settings is closer to it, as can be observed in **Figure 10**. It is suggested that the reason for the stiffer behaviour of the OM4IS optimal AHM can be the fact that only 50th percentile young men were tested in the lap belted OM4IS tests. It is therefore not surprising that the model responses are stiffer and may not represent variances in the occupant characteristics.

The results for the lateral lane-change do not differ to the same extent as for the frontal braking. A excellent CORA rating (0.96) for the OM4IS optimal parameter set and for the baseline settings (0.95)

is observed for this scenario. The differences between the responses of both parameter sets are small which suggests that both parameter sets could be applied in future work. Usually the belt system, in particular a 3-point belt system, has less contribution to the restraint of the occupant in lateral scenarios as the occupants just slips under the shoulder belt [11] [17] [30]. Consequently, compared to the frontal braking, it has a less effect to the variance of the lateral head COG excursions. The results also suggest that the effect of human bracing to the lateral excursions, whether consciously through tension or unconsciously through reflexes, is low compared to frontal scenarios. The results of the centre console width study support this hypothesis, as the gap increase of 20mm between the console and occupant increases the lateral head excursion by 10mm.

Hence, it is suggested that in future vehicles with rotated seat arrangements care must be taken especially for the lateral guidance of occupants to limit the lateral head excursions by for example the seat structure. Following the same logic, the investigated combined scenario, right turn with braking, shows comparable good results as the braking and lane-change, while the previously discussed aspects stay valid here too. The results suggest that the Simcenter Madymo AHM can predict the human kinematics in a combined pre-crash scenario accurately, which is a prerequisite for the following discussion on the kinematics envelope in a rotated seat arrangement.

The fair rating for the UMTRI braking scenario using the OM4IS optimal parameter set has been considered when looking into the rotated seat arrangement using the 3-point seat belt. Therefore, the Simcenter Madymo Baseline parameter settings are used for that scenario as they provide a good (0.89) overall CORA rating for the UMTRI scenarios.

Comparing the kinematics response of the lap-belted to the 3-point belted occupant it is found that the later has a significant effect to the head motions in all considered deceleration directions except the backward cases where the occupant strikes the headrest. It limits in the case of the 0° frontal pulse the mean head motion to 125mm instead of 280mm which is a reduction of 55%. It is also effective in the lateral load cases: e.g. 45° the maximum lateral mean motion reduces from 285mm to 105mm (-63%) and in the case of 315° from 250mm to 115mm (-54%). This also suggests that the 3-point belt is more effective in the direction where the shoulder belt is on the shoulder, which offers optimisation potential trying to reduce this unbalanced restraint. However, in both scenarios the lateral motions are on approximately same height as the frontal motions. This suggests that even if the 3-point belt is overall more effective in restraining the occupant in a rotated seat arrangement pre-crash scenario, there is still potential to improve its performance. For example, an motorised seat belt system is found to be effective by improving the coupling of the occupant to the vehicle structure and therefore improved ride-down-effect in the successive crash phase [17] [31]. However, in addition to the belt system, the seat structure as central element of the restraint system, must also be considered as the lateral guidance of the occupant in the seat is found to be sensitive to the head displacements in the lateral direction. Thus, the application of another seat type, be it with a better or worse lateral guidance, may change the present results.

The pre-crash kinematics' envelope, or the enclosed space in which the occupant moves, as illustrated in **Figure 20** for 3-point belted, in **Figure 21** for lap-belted occupants and in **Figure 22** as comparison of both, is proposed as first step in considering those motions in the design of future airbag systems and vehicle cabin layouts. Recently, airbag systems which are integrated into the seat back and deploying from the back of the seat, over the head in front of the occupant are investigated, as well as deploying from the vehicle roof and integrated within the seatbelt [24]. These concepts have one thing in common: they might have the potential to work properly in terms of injury reduction for in-position scenarios but when the occupant is (dynamically) out-of-position (OoP), for example by experiencing a pre-crash manoeuvre before the airbag is triggered, their interaction with the occupant during deployment could

introduce injuries. Vehicle cabin layouts must be designed in a way to avoid occupant to interior or occupant to occupant contact due to the motion caused by pre-crash manoeuvres and the findings from this study provide the first step to address this challenging issue.

6 Conclusion

This paper presents a methodology to extract the occupants' head kinematics envelope during the pre-crash phase in an expected automated driving level 5 scenario.

The Simcenter Madymo AHM Version 3 was utilized and correlated to a lap-belted OM4IS data set for which volunteers' kinematics corridors were extracted in a vehicle subjected to frontal (emergency braking) and lateral (lane change) manoeuvres. This was achieved by optimising the AHMs' activation parameters CORA score from the standard AHM factory settings from 0.64 (fair) to 0.79 (good). These optimised parameters were then tested against another dataset from UMTRI, representing different occupant demographics (age, gender, BMI), seatbelt arrangement, as well as vehicle manoeuvres able to test the AHM's omnidirectional response. It was observed that in the UMTRI scenarios, the standard AHM settings were more accurate than the OM4IS optimised parameters (CORA 0.84 vs 0.82), however when considering the AHM's response independently of the seatbelt arrangement by combining the UMTRI and OM4IS results, the OM4IS parameters were more accurate (CORA 0.81 vs 0.74), i.e. more suited for future the study of occupants in future L5 autonomous vehicle scenarios. However, the fair CORA rating for the UMTRI braking scenario using the OM4IS optimal parameter was considered by using the Simcenter Madymo Baseline parameter settings, which scored 0.84 overall for the 3-point belted UMTRI scenario. Future improvements of the Simcenter Madymo AHM should address this challenge, i.e. improve the models' response to become more independent of the torso restraint.

The kinematics of an occupant in a L5 driving scenario, considering a 1g emergency braking with 360° seat orientation (with the backrest vertical -20°) and different seat belt configurations (3 point and lap-belt) were studied. It was observed that that the 3-point seat belt is more effective than the lap-belt in restraining the occupant during the pre-crash phase, e.g. in reducing the maximum frontal kinematics for the 0-degree impact by 200mm from 350mm to 150mm (including 1 σ). However, there is improvement potential, especially for the lateral restraint, because the motions in that direction are approximately the same as those in the frontal direction. This underlines the needs to improve the occupants' coupling to the seat structure. The dynamic OoP effects are particularly important when designing airbag systems deploying over the head or from the vehicle roof. Interactions of the occupants' head with a deploying airbag device are very likely to increase the risk of injury. The vehicle layout must also be considered. Contacts of the occupants' head to hard interior parts and contact between heads of different occupants is also very likely to increase the risk of injury too. These two possible increases in risk must therefore be avoided. The occupants' kinematics envelopes presented in this paper are the first step to define occupants' motion in L5 rotated seat arrangements and hence design safe airbag systems and vehicle cabin layouts.

7 Limitations and Future Work

The results are limited to the application of the Simcenter Madymo 50th percentile AHM, correlated to the OM4IS test and validated to the UMTRI tests supplemented with the activation parameters described in this paper. Both parameter settings, Madymo standard and OM4IS correlated, show a CORA rating of > 0.8 (good) at the end. However, a fair rating for the braking scenario using the OM4IS optimal parameter set in the validation to the UMTRI data must be considered when investigating scenarios using a torso restraining seat belt device. Future work could address this challenge, be it by improving the AHM model or by creating new, improved test databases.

The Simcenter Madymo baseline seat model is a standard seat model provided by SISS which is used in industry for concept design because of its realistic shape, dimensions and cushion stiffness [26]. The application of other seat models may change the presented results, especially for the lateral motions. The used pre-brake pulse for the rotated seat arrangement study is of generic type and the seat back angles others than the one used here (20°) are not considered. Further research is needed for other seat back angles (e.g. 40° for relaxed seating position) and variations of the seat lateral guidance. Additionally, it is proposed to investigate the effect of the pre-crash motion to the in-crash injury outcome.

8 Acknowledgements

This research did not receive any specific grant from funding agencies in the public, commercial, or not-for-profit sectors. The author would like to thank Siemens Industry Software Services B.V. (SISS) for providing the Simcenter Madymo license.

References

- [1] European Transport Safety Council, “2010 Road Safety Target Outcome: 100,000 fewer deaths since 2001,” p. 94, 2011.
- [2] European Commission, “What we do | Mobility and transport.” [Online]. Available: https://ec.europa.eu/transport/road_safety/what-we-do_en. [Accessed: 12-Jul-2020].
- [3] European Transport Safety Council, “New EU transport commissioner commits to halve road deaths and serious injuries by 2030.” [Online]. Available: <https://etsec.eu/new-eu-transport-commissioner-commits-to-halve-road-deaths-and-serious-injuries-by-2030/>. [Accessed: 12-Jul-2020].
- [4] J. Leohold, “Highly Automated Driving : Fiction or Future ?,” in *HAVEit Final Event*, 2011, p. 13.
- [5] D. Subit, P. Vezin, S. Laporte, and B. Sandoz, “Will automated driving technologies make today’s effective restraint systems obsolete?,” *Am. J. Public Health*, vol. 107, no. 10, pp. 1590–1592, 2017, doi: 10.2105/AJPH.2017.304009.
- [6] T. L. Mcmurry, G. S. Poplin, G. Shaw, and M. B. Panzer, “Crash safety concerns for out-of-position occupant postures : A look toward safety in highly automated vehicles Crash safety concerns for out-of-position occupant postures : A look toward safety,” *Traffic Inj. Prev.*, vol. 0, no. 0, pp. 1–6, 2018, doi: 10.1080/15389588.2018.1458306.
- [7] SAE international, “U.S. Department of Transportation’s New Policy on Automated Vehicles Adopts SAE International’s Levels of Automation for Defining Driving Automation in On-Road Motor Vehicles,” *SAE Int.*, p. 1, 2016, doi: P141661.
- [8] J.D. Power, “2019 Q3 Mobility Confidence Index Study fueled by SurveyMonkey Audience | J.D. POWER,” 2019. [Online]. Available: <https://www.jdpower.com/business/press-releases/2019-q3-mobility-confidence-index-study-fueled-surveymonkey-audience>. [Accessed: 14-Jul-2020].
- [9] S. Jorlöv, K. Bohman, and A. Larsson, “Seating positions and activities in highly automated cars - A qualitative study of future automated driving scenarios,” in *Conference proceedings International Research Council on the Biomechanics of Injury, IRCOBI*, 2017, vol. 2017-Septe.
- [10] V. Hasija and E. G. Takhounts, “SIMULATION ASSESSMENT OF INJURY TRENDS FOR 50TH PERCENTILE MALES USING POTENTIAL SEATING CONFIGURATIONS OF FUTURE AUTOMATED DRIVING SYSTEM (ADS) EQUIPPED VEHICLES,” *26th ESV Conf.*, vol. 0, pp. 1–13, 2019.
- [11] Y. Kitagawa, S. Hayashi, K. Yamada, and M. Gotoh, “Occupant Kinematics in Simulated Autonomous Driving Vehicle Collisions: Influence of Seating Position, Direction and Angle,” *Stapp Car Crash J.*, vol. 61, no. November, pp. 101–155, 2017.
- [12] K. Bohman, R. Örtlund, G. Kumlin Groth, P. Nurbo, and L. Jakobsson, “Evaluation of users’ experience and posture in a rotated swivel seating configuration,” *Traffic Inj. Prev.*, vol. 0, no. 0, pp. 1–6, 2020, doi: 10.1080/15389588.2020.1795149.
- [13] T. Matsushita, H. Saito, C. Sunnevång, M. Östling, A. Vishwanatha, and A. Tabhane, “Evaluation of the Protective Performance of a Novel Restraint System for Highly Automated Vehicles (Hav),” *26th ESV Conf.*, no. 2019, p. Paper No. 19-0321, 2019.
- [14] J. Zhao, M. Katagiri, S. Lee, and J. Hu, “GHBMC M50-O Occupant Response in A Frontal Crash of Automated Vehicle,” in *HUMAN MODELING AND SIMULATION IN AUTOMOTIVE ENGINEERING 2018*, 2018, pp. 1–20.
- [15] C. Bastien, “the Prediction of Kinematics and Injury Criteria of Unbelted Occupants Under Autonomous Emergency Braking,” Coventry University, 2014.
- [16] T. Matsuda, K. Yamada, S. Hayashi, and Y. Kitagawa, “Simulation of Occupant Posture Changes due to Evasive Manoeuvres and Injury Predictions in Vehicle Frontal and Side Collisions,” in *IRCOBI Conference 2018*, 2018, pp. 512–523.

- [17] S. Battaglia, K. Kietlinski, M. Unger, R. van der Made, and R. Bours, "Occupant Behavior during a One-Lane Change Maneuver resulting from Autonomous Emergency Steering," in *23th ESV Conference*, 2013, pp. 1–13.
- [18] Siemens Industry Software and Services B.V., "Human Body Models Manual," 2017.
- [19] A. Diederich, "Validation of Computational Human Body Models for the Assessment of Occupant Safety," 2018.
- [20] C. Bastien, M. V. Blundell, and C. Neal-Sturgess, "A study into the kinematic response for unbelted human occupants during emergency braking," *Int. J. Crashworthiness*, vol. 22, no. 6, pp. 689–703, 2017, doi: 10.1080/13588265.2017.1301080.
- [21] C. Gehre, H. Gades, and P. Wernicke, "Objective Rating of Signals using Test and Simulation Responses," in *21th ESV Conference*, 2009, p. 8.
- [22] S. Kirschbichler *et al.*, "Factors Influencing Occupant Kinematics during Braking and Lane Change Maneuvers in a Passenger Vehicle," in *IRCOBI Conference 2014*, 2014, pp. 614–625.
- [23] P. Huber, S. Kirschbichler, A. Pruggler, and T. Steidl, "Passenger kinematics in braking, lane change and oblique driving maneuvers," in *IRCOBI Conference 2015*, 2015, pp. 783–802.
- [24] M. Östling, A. Larsson, H. Wu, and C. Sunnevång, "Driver Behaviour in Automated Vehicles and Effects on Safety – A Swedish and Chinese perspective How do we save more lives in the future?," in *VDI Safety Systems 2018*, 2018.
- [25] M. P. Reed, S. M. Ebert, B. D. Park, and M. L. H. Jones, "Passenger Kinematics During Crash Avoidance Maneuvers," Ann Arbor, 2018.
- [26] Siemens Industry Software and Services B.V., "Model Manual of the MADYMO Application Model for Integrated Safety," 2018.
- [27] M. Östling, H. Saito, A. Vishwanatha, C. Ding, B. Pipkorn, and C. Sunnevång, "Potential benefit of a 3+2 criss cross seat belt system in frontal and oblique crashes," *Conf. Proc. Int. Res. Counc. Biomech. Inj. IRCOBI*, vol. 2017-Sept, no. 0, pp. 390–409, 2017.
- [28] S. Ejima, Y. Zama, K. Ono, K. Kaneoka, I. Shiina, and H. Asada, "Prediction of pre-impact occupant kinematic behavior based on the muscle activity during frontal collision," in *21th ESV Conference*, 2009.
- [29] K. Devane, D. Johnson, and F. S. Gayzik, "Validation of a simplified human body model in relaxed and braced conditions in low-speed frontal sled tests.," *Traffic Inj. Prev.*, vol. 0, no. 0, pp. 1–6, 2019, doi: 10.1080/15389588.2019.1655733.
- [30] R. Meijer, C. Rodarius, J. Adamec, E. Van Nunen, and L. Van Rooij, "A first step in computer modelling of the active human response in a far-side impact," *Int. J. Crashworthiness*, vol. 13, no. 6, pp. 643–652, 2008, doi: 10.1080/13588260802296015.
- [31] K. Yamada, M. Gotoh, Y. Kitagawa, and T. Yasuki, "Simulation of Occupant Posture Change during Autonomous Emergency Braking and Occupant Kinematics in Frontal Collision," in *IRCOBI Conference 2016*, 2016, pp. 261–274.

Appendices

A. Kinematics Corridors for Emergency Braking and Lane Change (OM4IS Data)

Kinematics Corridors for Emergency Braking:

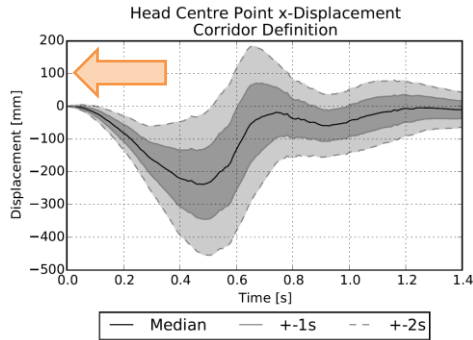


Figure 23. Emergency Braking: Reaction Corridors for the Head Centre Point x-displacement.

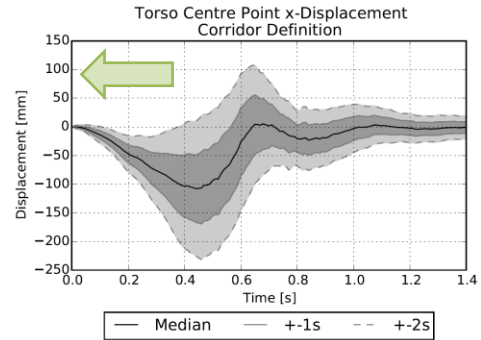


Figure 24. Emergency Braking: Reaction Corridors for the Torso Centre Point x-displacement.

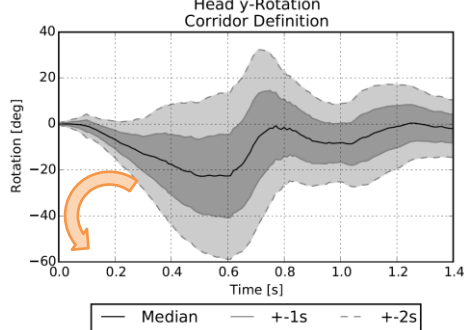


Figure 25. Emergency Braking: Reaction corridors for the Head Centre Point y-rotation.

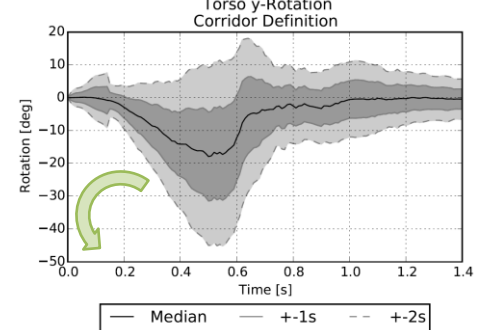


Figure 26. Emergency Braking: Reaction corridors for the Torso Centre Point y-rotation.

Kinematics Corridors for Lane-Change:

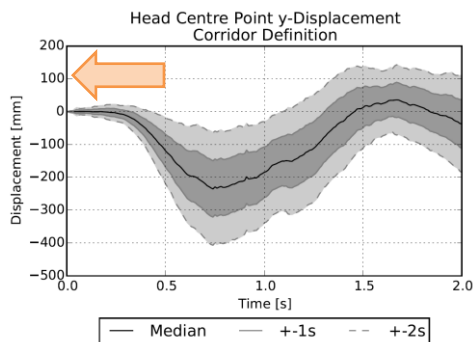


Figure 27. Lane-Change: Reaction Corridors for the Head Centre Point y-displacement.

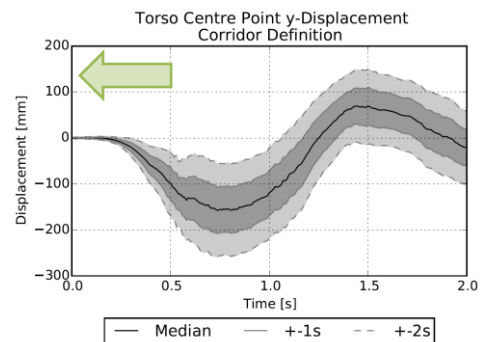


Figure 28. Lane-Change: Reaction Corridors for the Torso Center Point y-displacement.

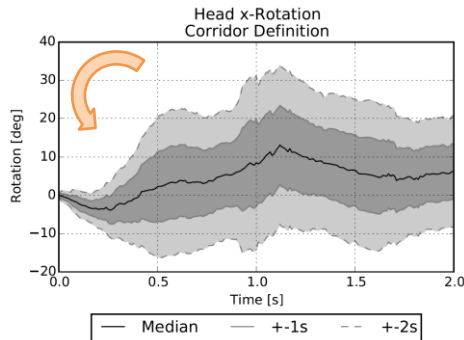


Figure 29. Lane-Change: Reaction Corridors for the Head Centre Point x-rotation.

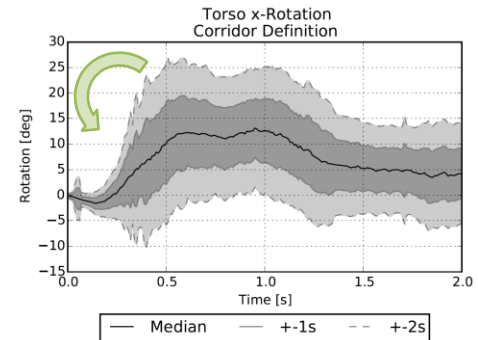


Figure 30. Lane-Change: Reaction Corridors for the Torso Centre Point x-rotation.

B. OM4IS Emergency Braking Kinematics Comparison of the Master Parameter Settings with a Median Response Volunteer

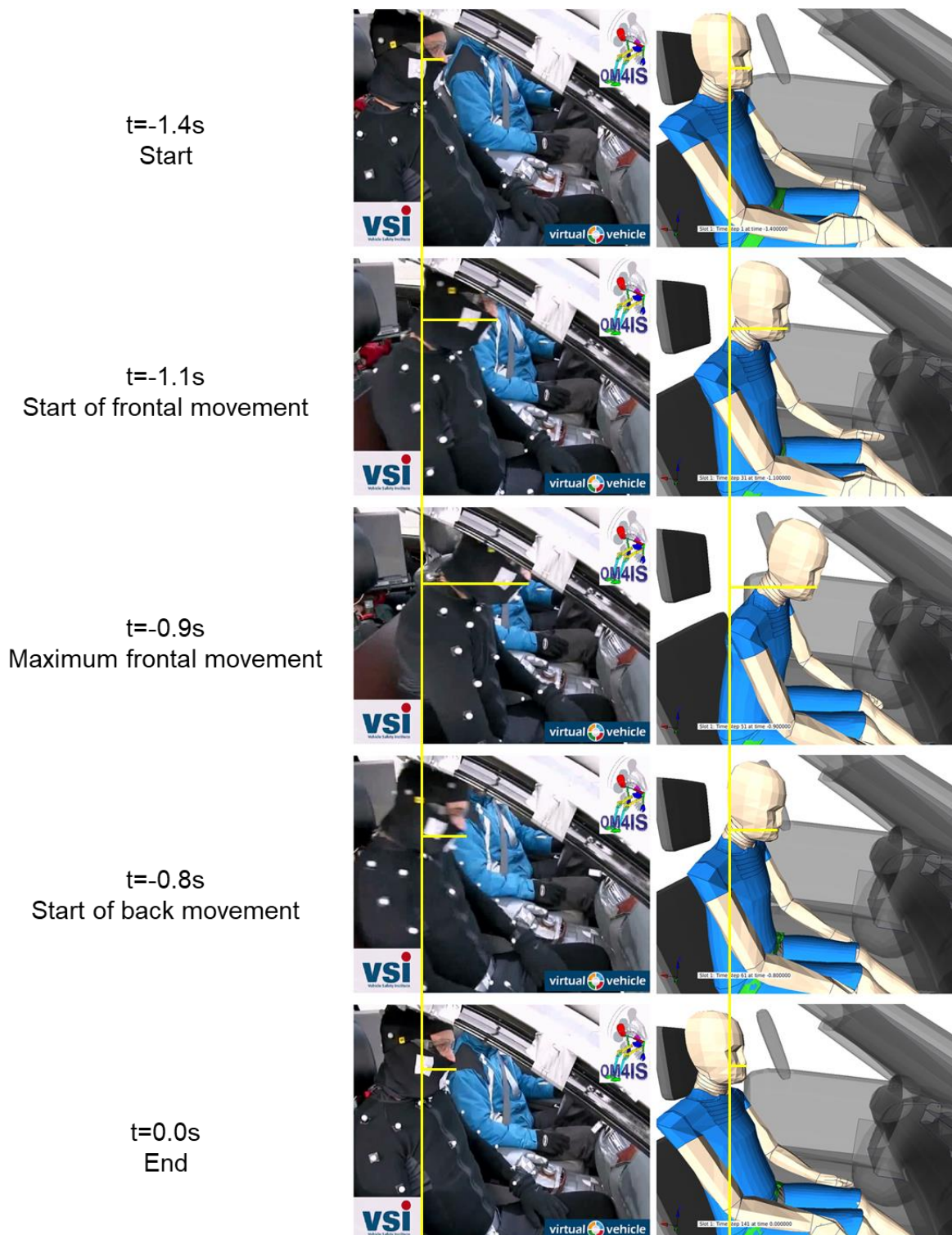


Figure 31. OM4IS Emergency Braking Kinematics Comparison of the Master Parameter Settings with a Median Response Volunteer

C. OM4IS Lane-Change Kinematics Comparison of the Master Parameter Settings with a Median Response Volunteer

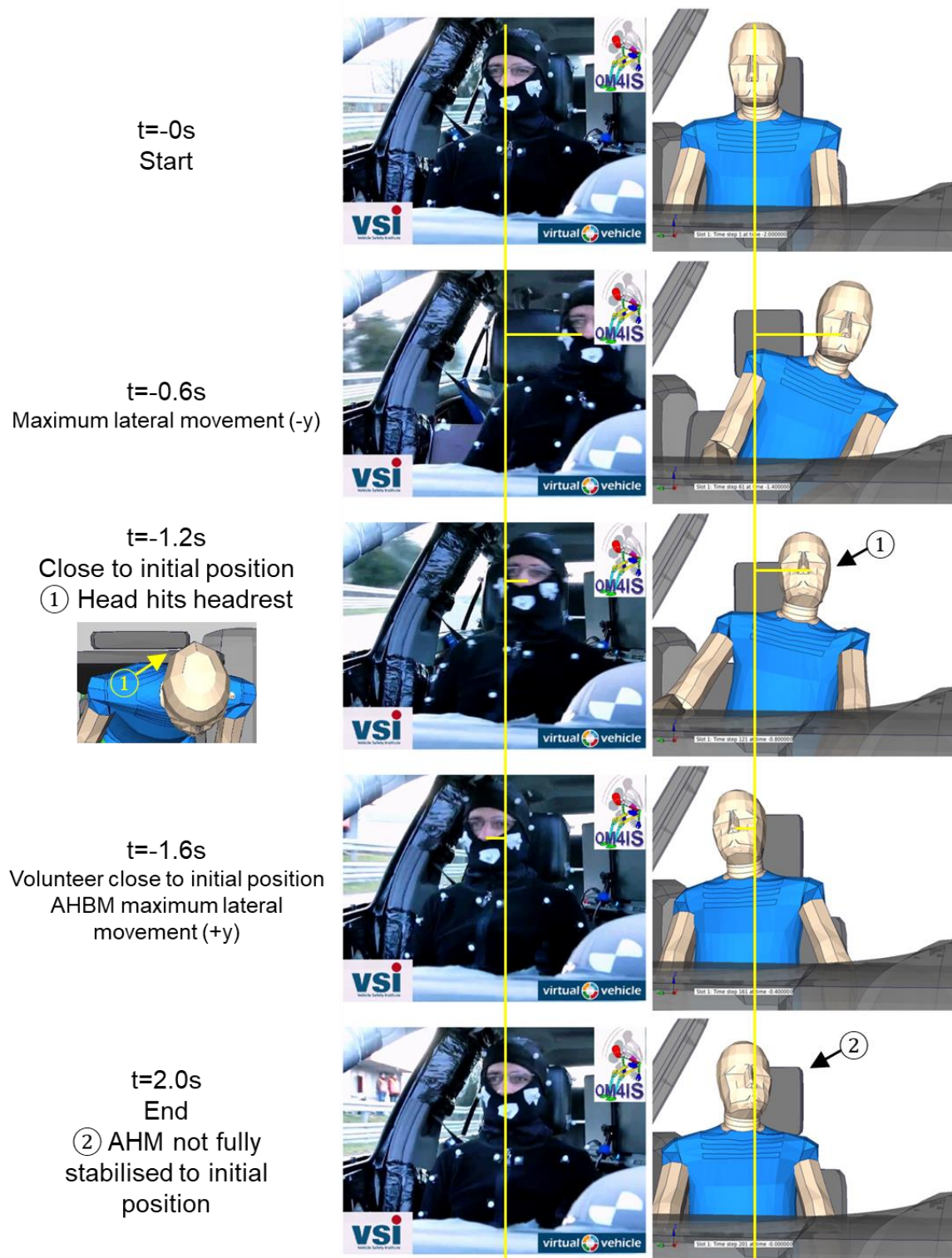


Figure 32. OM4IS Lane-Change Kinematics Comparison of the Master Parameter Settings with a Median Response Volunteer

D. UMTRI Kinematics Comparison for the Braking and Lane-Change Event

Kinematics Comparison for the Braking Event:

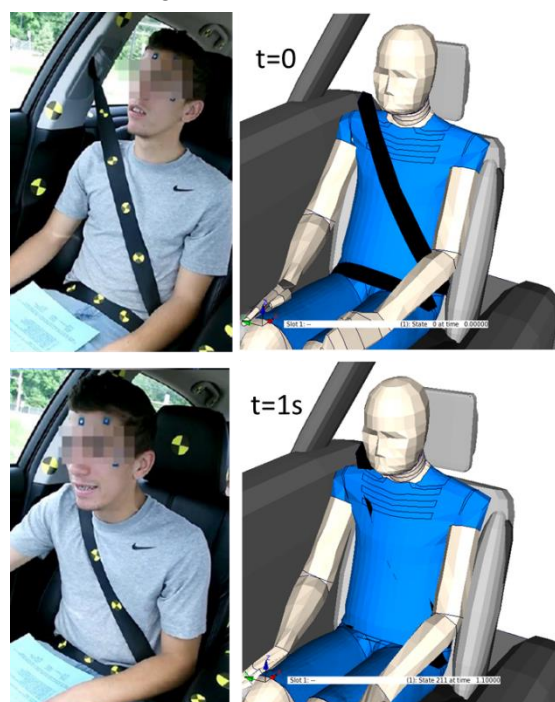


Figure 33. Kinematics Comparison for the UMTRI Braking Event

Kinematics Comparison for the Lane-Change-Event:

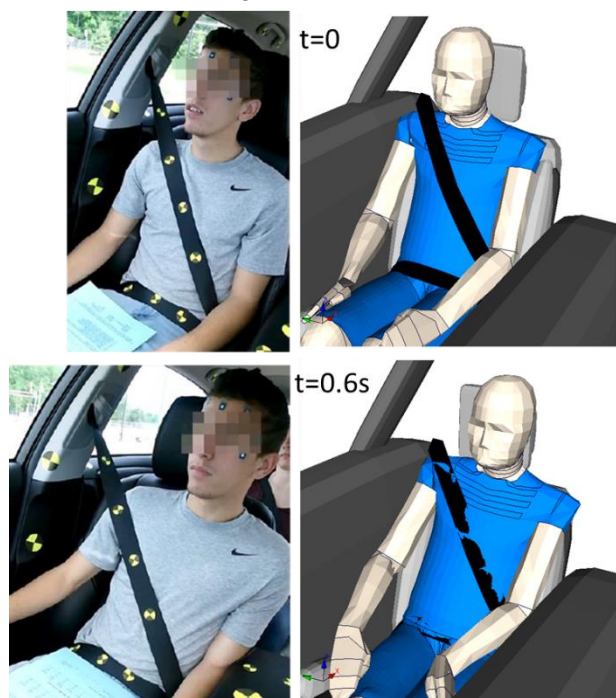
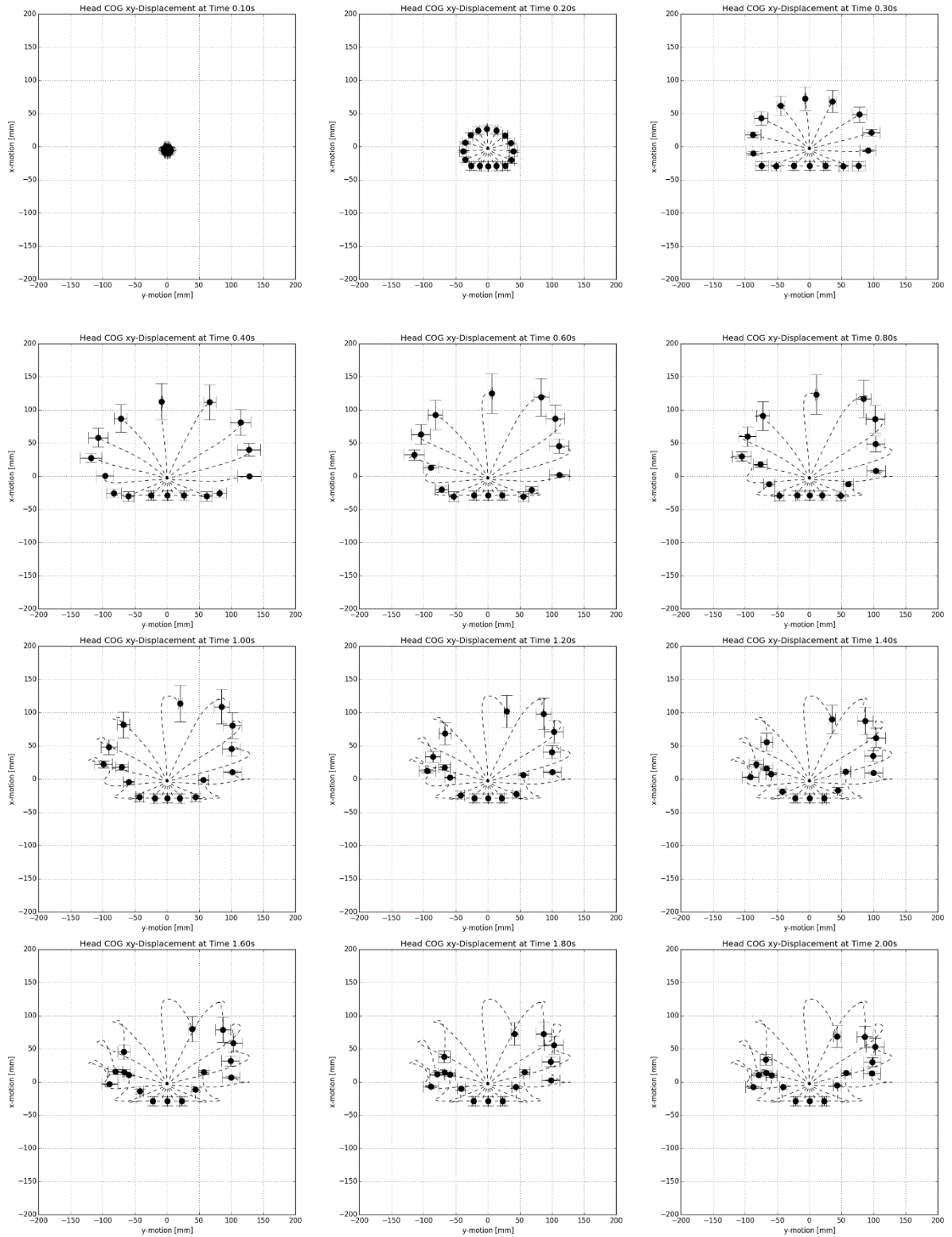


Figure 34. Kinematics Comparison for the UMTRI Lane-Change Event

E. Head COG Kinematics in the xy-Plane for the 3-point belted Occupant

Head COG xy-displacement for the 3-point belted occupant starting at $t = 0.1\text{s}$ in steps of 0.1s until $t = 0.4\text{s}$, afterward is steps of 0.2s until $t = 2.0\text{s}$:



F. Head COG Kinematics in the xy-Plane for the lap-belted Occupant

Head COG xy-displacement for the lap-belted occupant starting at $t = 0.1s$ in steps of $0.1s$ until $t = 0.4s$, afterward is steps of $0.2s$ until $t = 2.0s$:

